RSC Advances

REVIEW

View Article Online
View Journal | View Issue

Cite this: *RSC Adv.*, 2026, **16**, 24095

Photocatalysts for the decarboxylation conversion of C(sp^3)-carboxylic acids: a review

Changwen Gao, Jiasheng Zhang, Guangsong Li and Hongjian Peng *

Received 18th February 2026
Accepted 26th March 2026

DOI: 10.1039/d6ra01440b

rsc.li/rsc-advances

C(sp^3)-carboxylic acids are derived from a broad spectrum of sources and possess excellent biosafety. Its decarboxylation conversion provides an important route for constructing C–H, C=C and C–X (X = C, O, and F) bonds. Photocatalysis provides a mild and efficient method for achieving this conversion. In this paper, the photocatalysts used in the decarboxylation of C(sp^3)-carboxylic acids over the past 8 years are systematically reviewed. They are classified into four categories: organic transition metal complexes, simple transition metal salts, metal-free homogeneous photocatalysts and semiconductor material photocatalysts. The structural characteristics, catalytic principles and reaction mechanisms of various catalysts are described in detail, and the core reaction paths of different catalytic systems are analyzed. The advantages and disadvantages of various catalysts in terms of catalytic efficiency, substrate applicability, cost and recovery were compared. Finally, the key challenges in this field are pointed out, and the future development directions, such as the design of near-infrared light-responsive catalysts and the improvement of quantum efficiency, are proposed.

1. Introduction

C(sp^3)-carboxylic acids are abundant in nature (*e.g.*, amino acids, fatty acids, and sugar acids) and play key roles in organic synthesis and biodiesel production. The world produces 181.5 billion tons of lignocellulosic biomass every year, with only about 8.2 billion tons of biomass being utilized. The difficult degradation and structural complexity of lignocellulose have greatly hampered its effective utilization. Carbohydrates can usually be obtained from various biomass raw materials by enzymes or acids, and then further converted into biomass-derived platform compounds.[1,2] In addition, waste edible oils (WCO) and low-value by-products from petroleum processing and papermaking contain large amounts of fatty acids,[3–9] which are readily available at low cost for biodiesel production *via* hydrodecarboxylation. Using these materials can not only realize the comprehensive utilization of waste and provide safe, efficient and renewable energy but also eliminate potential risks to food safety and deliver good economic benefits. For example, a hydrogen-enriched Pt/TiO_2 catalyst can convert C_{12}–C_{18} fatty acids from biological sources into C_{n-1} alkanes with high selectivity under mild conditions, and the yield can exceed 90%, making it suitable for industrial low-value fatty acid mixtures such as soybean oil and rosin oil.[10] By constructing a hydrogen-deficient catalytic interface, a Ru/TiO_2 catalyst enabled the decarboxylative coupling reaction of fatty acids, generating long-chain alkanes and simultaneously producing hydrogen, thereby improving energy utilization efficiency.[11] Photocatalysis (using fatty acid photodecarboxylase (FAP)), combined with a membrane reactor, enables continuous flow production, enhances catalytic stability and reusability, and provides technical support for large-scale production.[12] In addition, carboxylic acids have not only been widely commercialized but also exhibit less toxicity and higher stability during organic synthesis compared to more reactive coupling partners (such as halides or organic metals).[13–18] Photocatalytic decarboxylation is emerging as an effective method for generating C–H, C=C and C–X (X = C, O or F) bonds *via* free radical processes under mild reaction conditions. Introducing visible light into the decarboxylation reaction can promote the chemoselective activation of molecular substrates. This broadens the scope for designing and discovering new chemical transformations.[19–24] Covalent organic framework (COF)-based photocatalysts have been used in the decarboxylative fluorination reaction to enable the post-functionalization of anti-inflammatory drugs and steroid derivatives.[25] The cobalt–cerium synergistic photocatalytic strategy is used for the decarboxylation Heck reaction of fatty acid substrates, which is suitable for the late modification of active drug molecules, and the by-products are environmentally friendly hydrogen and carbon dioxide.[26] The iron/copper dual catalytic system supports the decarboxylative amination and alkylation of a variety of complex drugs and natural products, which is helpful for the rapid construction of drug libraries and the discovery of new drugs.[27] These studies have shown that photocatalytic decarboxylation provides an efficient, mild and environmentally friendly strategy for the synthesis and modification of drug skeletons.[28] However, current photocatalysis still

College of Chemistry and Chemical Engineering, Central South University, Changsha, Hunan 410083, China. E-mail: hongjianpeng@126.com

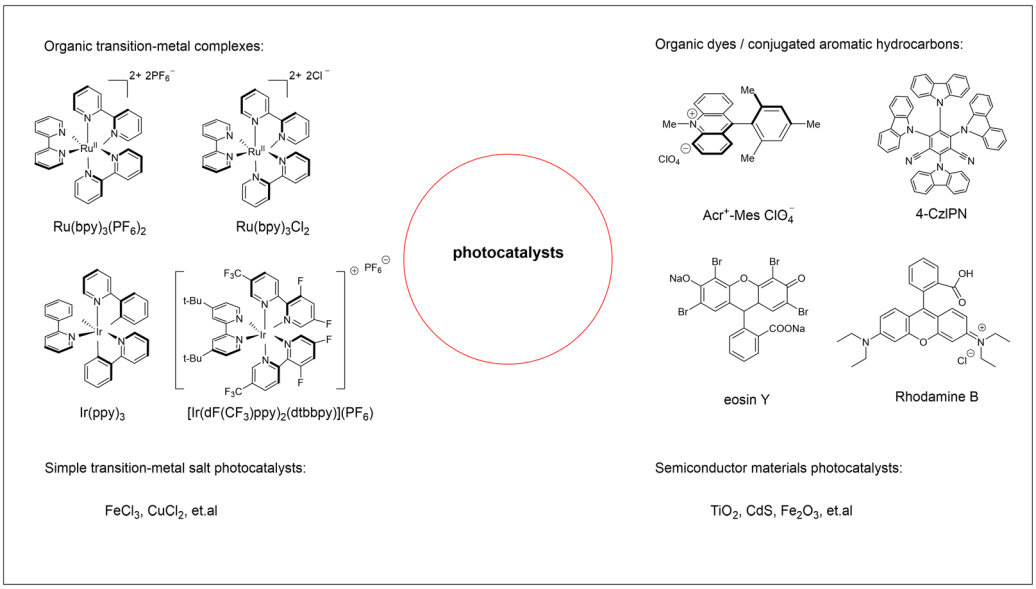

Fig. 1 Typical photocatalysts for decarboxylation conversion.

faces many problems, such as the lack of cheap, suitable green photocatalysts and high time consumption due to low catalytic efficiency. These are all urgent problems to be solved.[29–32] In the past few decades, many efforts have been devoted to the direct decarboxylation of C(sp^3)-carboxylic acids without extra pre-activation to generate carbon-centered free radicals.[33–37]

Based on previous studies, different kinds of photocatalysts have been reported (Fig. 1), mainly including organic transition-metal complexes (noble metal Ru, Rh, Ir complexes),[38,39] simple transition metal salt photocatalysts ($FeCl_3$, $CuCl_2$, *etc.*),[40,41] metal-free photocatalysts such as organic dyes/conjugated aromatic hydrocarbons (*e.g.*, eosin, acridine, and polycyanoarenes)[42–45] and semiconductor materials (TiO_2, CdS, ZnO, *etc.*).[46,47] According to the different roles of these types of photocatalyst materials in the decarboxylation reaction, four mechanisms are summarized in Scheme 1.[48–52] In the first mode, the carboxylate is oxidized by the excited photocatalyst, and a carboxyl radical is generated *via* single-electron transfer (SET). This radical spontaneously releases carbon dioxide and simultaneously forms a carbon-centered radical (Scheme 1a). The second mode involves ligand exchange between carboxylic acids and metal salts to form ground-state carboxylates. Subsequently, these carboxylates are excited under light and undergo homolysis *via* ligand-to-metal charge transfer (LMCT), producing carboxyl radicals and low-valent metal centers. Alkali is essential for the first two modes (Scheme 1b). The third mode is called the proton-coupled electron transfer (PCET) process. In this mode, electron transfer and proton coupling work together. Hydrogen bond complexes are formed between the carboxylic acid and photocatalyst (acridine), and photoexcited states are generated under visible light irradiation. After the photocatalyst accepts electrons, the negative charge density increases, which just promotes proton binding. The proton binding stabilizes the negative charge and reduces the energy barrier of the next electron transfer. The result is to generate carboxyl radicals by homolysis. The advantage of using this catalyst is that it not only has a low oxidation potential, but also does not require the participation of alkali (Scheme 1c). The fourth mode is a semiconductor photocatalyst, and its catalytic mechanism is significantly different from the first three. Taking TiO_2 catalyst as an example, it can absorb photons with energy higher than the semiconductor's band gap and then excite electrons to the conduction band (CB) and create holes in the valence band (VB). Holes formed in the valence band exhibit strong oxidizing ability; they can oxidize carboxylates to form carboxyl radicals. Carboxyl radicals spontaneously release CO_2 and simultaneously form carbon-centered radicals (Scheme 1d). The most prominent advantage of this kind of photocatalyst is that it is a kind of heterogeneous phase, which is convenient for subsequent separation from the products.

2. Organic transition-metal complexes

Organic transition-metal complexes that harvest visible light now underpin a large fraction of modern photocatalysis, enabling mild radical chemistry, C–C/C–heteroatom bond formation, and polymerization. Transition-metal complexes (Ru, Ir, Cu, Co, Pd, Pt, first-row metals) absorb visible light to reach long-lived excited states that participate in SET, energy transfer (EnT), atom transfer, or inner-sphere radical processes.[53,54] Classical $Ru(bpy)_3^{2+}$/Ir(III) complexes operate mainly *via* outer-sphere SET, while newer Mn/Co/Cu/Pd systems use photoinduced inner-sphere mechanisms where substrate–metal binding is crucial. Pd, Co and Pt complexes can act simultaneously as chromophore and cross-coupling catalysts, redirecting oxidative addition into radical pathways and enabling stereodivergent or previously inaccessible transformation.[55–57] The activity and selectivity of organic transition metal complexes for photocatalytic decarboxylation

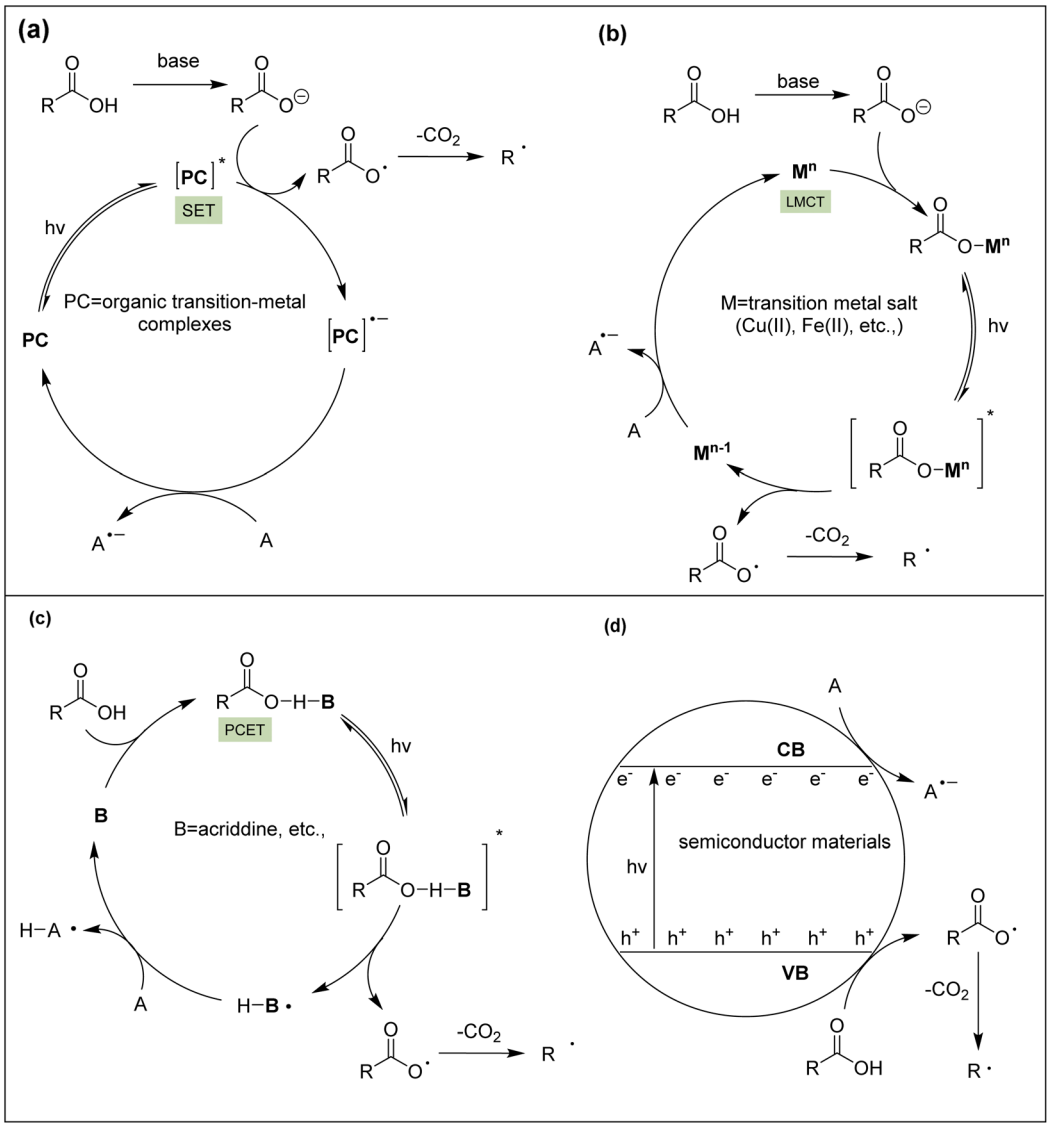

Scheme 1 Four mechanisms of the photocatalytic decarboxylative reaction. (a) SET, single-electron transfer. (b) LMCT, ligand metal charge transfer. (c) PCET, proton-coupled electron transfer. (d) general catalytic mechanism of semiconductor photocatalysts. (This figure has been adapted/reproduced from ref. 22 with permission from Royal Society of Chemistry, copyright 2025).

mainly depend on the electronic structure of the metal center and its interaction with the ligand. Light excitation causes the metal complex to enter the excited state and change its redox potential, thereby promoting the electron transfer process and generating carbon radicals to achieve the decarboxylation reaction. The electron recombination of this excited state is a key step. By adjusting the ligand structure and replacing the central metal atoms, the redox potential can be finely regulated to match the reaction requirements. But such photocatalysts usually require expensive precious metals and ligands and are not easily separated and recovered in the later stage, which limits their large-scale application in terms of cost.

In 2018, the Ritter group used $Ir[dF(CF_3)ppy]_2(dtbbpy)PF_6$ as a photocatalyst and $Co(dmgH)_2(4\text{-OMe-py})Cl$ as a proton reduction catalyst to achieve the first dehydrogenative decarboxylative olefination of carboxylic acids without stoichiometric additives.[58] The production of olefins from carboxylic acids by decarboxylation is a two-electron oxidation process of the carbon chain. Therefore, hydrogen must be released in the absence of stoichiometric oxidants. The study harnesses the reducing ability of the Co(III) complex ($E_{1/2}^{red}$ [Co^{III}/Co^{II}] = −0.68 V *versus* the saturated calomel electrode (SCE) in MeCN), stronger than the photoexcited iridium catalyst ($E_{1/2}^{red}$ [$Ir^{IV}/*Ir^{III}$] = −0.89 V *versus* the SCE in MeCN). The result is the formation of a Co(II) complex and a highly oxidizing Ir(IV) complex ($E_{1/2}^{red}$ [Ir^{IV}/Ir^{III}] = 1.69 V *versus* SCE in MeCN). The Co(II) complex is then ready to accept alkyl radicals formed by the decarboxylative oxidation of alkyl carboxylates by Ir(IV) to generate the Co(III) complex. During photodegradation, the cobalt–carbon bond is split, and the Co(III) compound is subjected to β-hydrogen capture to form olefins and Co(III) hydrides. The Co(III) hydride is protonated by carboxylic acid, and then the Co(III) catalyst is regenerated to complete the catalytic cycle (Scheme 2a). Enzymatic and chemical catalytic reactions are usually carried out

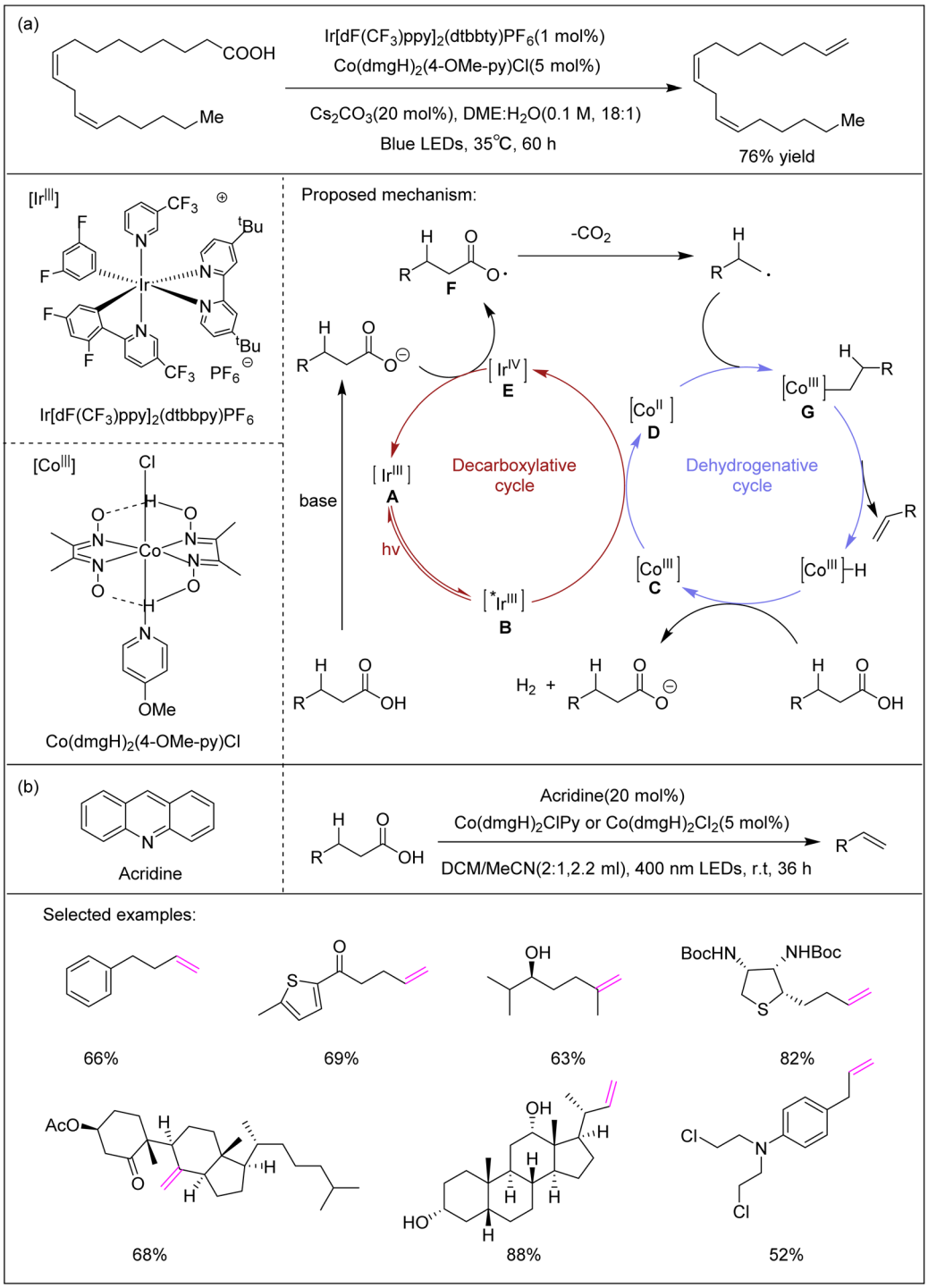

Scheme 2 (a) Photocatalytic decarboxylative elimination reported by the Ritter group. (This figure has been adapted/reproduced from ref. 58 with permission from Springer Nature, copyright 2018). (b) Acridine/cobalt oxime dual catalytic system proposed by the Nguyen group. (This figure has been adapted/reproduced from ref. 59 with permission from the American Chemical Society, copyright 2019).

under incompatible conditions. For example, enzymatic reactions are carried out in aqueous solutions at near room temperature and at a controllable pH, while chemical catalytic reactions may require anhydrous conditions and high temperature. Therefore, the synergistic chemoenzymatic catalytic process is still relatively rare and only suitable for a few reactions. In 2019, the Nguyen and colleagues developed a "triple catalytic system" (LACo) that combines photocatalysis and enzyme catalysis (double photocatalysis and enzyme catalysis), which is achieved through the coupling of the photoinduced acridine-catalyzed O-H-HAT and cobalt oxime-catalyzed C-H-HAT process.[59] The reaction realizes the HAT of the O–H bond through proton-coupled electron transfer (PCET) to generate acridine radicals (HA$^{\bullet}$) and carboxylate radicals (Scheme 2b).

This mechanism avoids strong alkaline conditions and a high redox potential, allowing the chemical process to coexist with enzymes (enzymatic reactions). In addition, it is known that the unsubstituted acridine affects the HAT process (BDE 112 kcal mol^{-1}) through a strong O–H bond, and its photocatalytic performance can be adjusted by introducing an alternative group to the pyrimidine core to form a new type of organic photocatalyst different from the traditional metal (Ru, Ir) or acridinium catalyst. The gram-scale verification is suitable for unrefined biomass.

In 2018, MacMillan and co-workers developed an integrated strategy of "open-shell radical-closed-shell metal migration–insertion".[60] Thus, the selective intermolecular addition of nucleophilic free radicals to inactivated alkynes was realized. The authors proposed the following mechanism (Scheme 3a): *N*-Boc-proline deprotonates, and the resulting carboxylate undergoes single-electron oxidation by Ir(III)* **B** to generate alkyl radical **C** and the reduced Ir(II) **D**. The open-shell alkyl species **E** is anticipated to quickly undergo oxidative radical capture with low-valent nickel species **F**, forming alkyl-Ni(II) complex **G**. This nucleophilic Ni(II) intermediate is then poised to undergo the

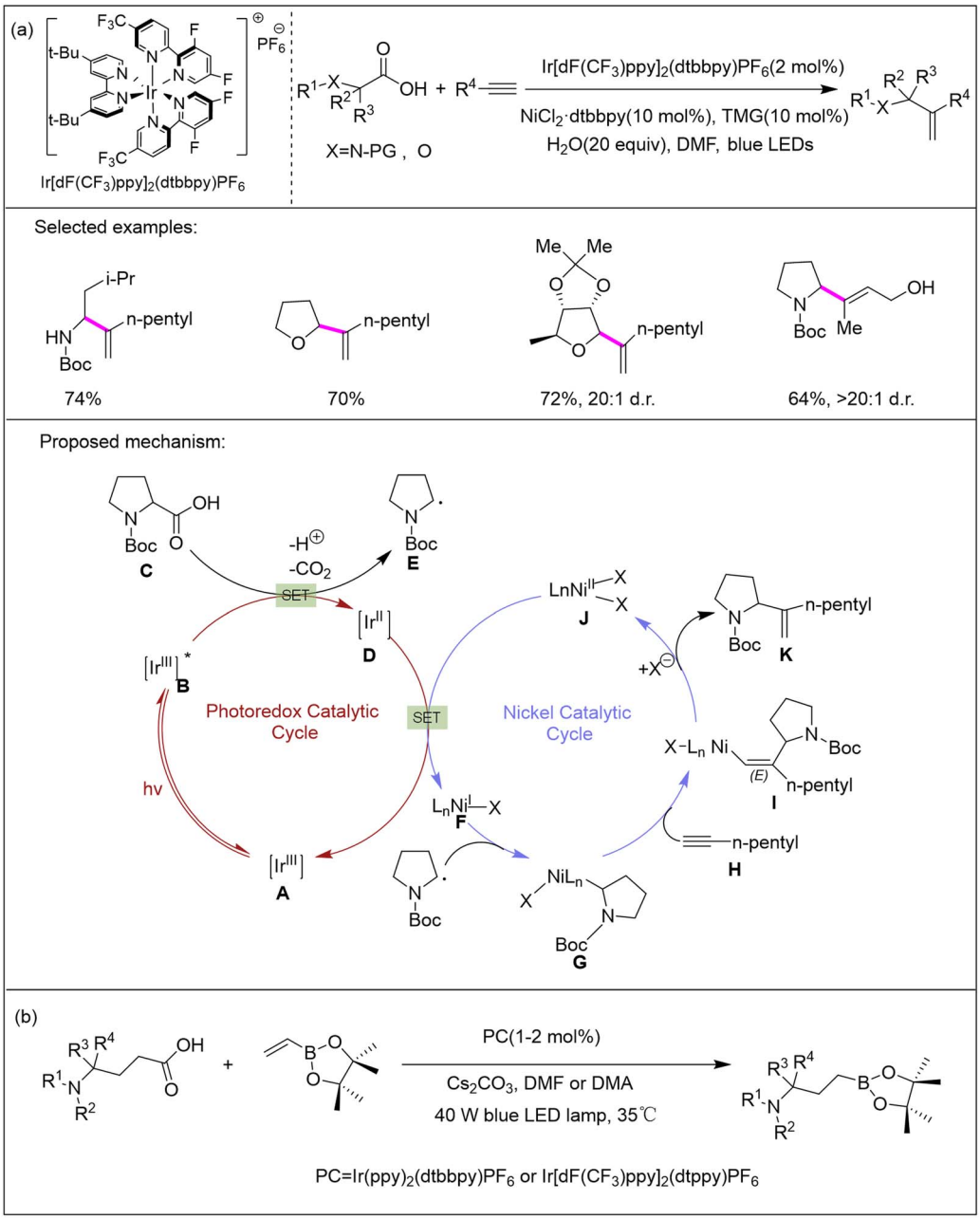

Scheme 3 (a) Decarboxylative addition reaction based on a nickel/photoredox dual catalytic system reported by the MacMillan group. (This figure has been adapted/reproduced from ref. 60 with permission from the American Chemical Society, copyright 2018). (b) Decarboxylative radical addition reaction of γ-amino acids with vinyl borates. (This figure has been adapted/reproduced from ref. 61 with permission from Wiley, copyright 2018).

crucial migratory insertion coupling step with alkyne **H**, generating the vinyl–nickel complex **I**. Finally, protodemetalation by either a protonated base or carboxylic acid would afford the $C(sp^3)$–$C(sp^2)$ coupled product K. The hydrogen alkylation reaction of various asymmetric acetylene systems exhibits excellent regional control, and its selectivity comes from the preference of alkyl migration insertion: the nickel center tends to be located at the sp carbon site with the highest electron cloud density in the alkyne, while the introduced alkyl is located at the highest electrophilic point based on the potential polarity of the alkyne. In addition, compared with the reaction products of sterically hindered asymmetric alkynes, the introduced alkyl groups are preferentially located at sites far from the large substituents of alkynes. In the same year, the Aggarwal group efficiently synthesized γ-amino borates by directly using readily available carboxylic acids (*e.g.*, γ-amino acids) and vinyl borates.[79] Deuterium labeling experiments and DFT calculations show that the reaction mechanism involves the single-electron reduction process of α-boryl radicals by reduced photocatalysts. This method exhibits excellent functional group tolerance to a variety of substrates (including natural products and drug skeletons). Importantly, this method can rapidly synthesize alkyl borates with diverse structures, which is of great value for pharmaceutical chemistry (Scheme 3b).

In 2020, the Rueping group utilized a similar catalytic system to realize the anti-Markovnikov regioselective alkylation of terminal alkynes with alkyl carboxylic acids (*e.g.*, amino acid derivatives) (Scheme 4a).[62] The energy barrier for the migration of the alkyl from the Ni center to the terminal carbon atom of the alkyne is only 6.3 kcal mol^{-1} (transition state B-TS), which is much lower than the path of migration to the internal carbon atom (16.8 kcal mol^{-1}, B-TS′), explaining the *anti*-Markovnikov selectivity. At the same time, a one-pot three-component coupling reaction was developed, enabling the efficient synthesis of trisubstituted olefins *via* the synergistic reaction of aryl bromides, alkyl carboxylic acids, and terminal alkynes (Scheme 4b). Finally, gram-scale synthesis (2.0 mmol) was successfully achieved, even for compounds with complex structures, such as steroids and heterocycles. The Ernouf group developed a method for obtaining functionalized 1,3-disubstituted cyclobutane (Scheme 4c).[63] Compared with the high abundance of cyclohexane and cyclopropane in commercially available drugs, the frequency of cyclobutane is lower.[64] The bicyclo[1.1.0]butane (BCB) framework has a very high ring strain energy (64 kcal mol^{-1}), and its central carbon–carbon bond has high p orbital characteristics, which can be used as a substitute for the corresponding olefins. The Giese-type addition reaction of the $C(sp^3)$ center radical with high-tension bicyclo[1.1.0]butane was realized by photochemical strain release drive. The strong reducible excited-state photocatalyst oxidizes a carboxylate Ir(III) complex ($E^*_{1/2} = -1.21$ V) by SET to generate free radicals. The radical addition initiates the heterolytic cleavage of the central bond of the BCB skeleton, accompanied by a huge tension release (calculated to show a stabilization energy of about 38.9 kcal mol^{-1}). This process provides a strong thermodynamic driving force, overcomes the kinetic energy barrier of the radical addition step, and makes the reaction irreversibly push toward the product direction. This method has significant practicability and can be directly used for the late cyclobutylation of complex molecules, providing a tool for pharmaceutical chemistry to expand chemical space. In the same year, the Sun group used O_2 as a green oxidant, Cs_2CO_3 as a base, and Ir[(dF(CF$_3$)ppy)$_2$(dtbpy)]PF_6 as a photocatalyst to develop a universal carboxylic acid decarboxylation and hydroxylation method.[65] The mechanism of this reaction is consistent with the SET of general organic transition metal complexes (Scheme 4d). It is worth noting that when $NaBH_4$ is added at the end of the reaction, the target alcohol yield is only 65%; in contrast, the addition of $NaBH_4$ before the start of the reaction increased the yield to 99%. This is due to the instability of the peroxy radicals generated during the reaction, resulting in a limited range of substrates. Through the role of *in situ* reducing agent $NaBH_4$, the free radical intermediates can be stabilized, which improves the yield and broadens the substrate range. Thus, different sp^3-hybridized carbon-containing carboxylic acids have been successfully used as substrates, including substituted phenylacetic and aliphatic carboxylic acids.

In 2021, Terrett and co-workers proposed a method for the synthesis of alcohols in a mixed solvent system of dichloroethane (DCE) and hexafluoroisopropanol (HFIP), using $[Ru(dtbbpy)_3](PF_6)_2$ combined with an iodine(III) oxidant, 2-toluenesulfonyl-2,3-dihydrobenzimidazole acetate, to directly generate carbocations from benzyl carboxylic acids, followed by alcohol or water molecule capture to achieve C–O coupled products.[66] This method uses an organic iodine photooxidation system but does not involve peroxide intermediates after decarboxylation. Instead, it innovatively uses the free radical-polar cross (RPC) mechanism to shift the decarboxylation reaction from the traditional free radical path to the carbocation path (Scheme 5). This method overcomes the limitation that carbon radicals produced by photoredox decarboxylation cannot directly react with nucleophilic alcohols. This is different from the known hydroboration process and is milder than the hydration conditions of standard olefins. This platform is also suitable for the decarboxylation of carbocations with C, N, and X (halogen) atom nucleophiles to achieve carbon–carbon and carbon–heteroatom coupling.

γ-Methylene-δ-valerolactone (GMDV) is a multifunctional C4-ring ligand notable for its role in the palladium-catalyzed decarboxylative *O*-allylation of phenols, where it efficiently forms Csp^3–O bonds under mild conditions, demonstrating high selectivity and efficiency as an allylation reagent.[67] GMDV also participates in phenol-mediated decarboxylative proton transfers to produce polysubstituted (E)-2,4-pentadienoates with excellent yields and stereoselectivity, highlighting its versatility in organic syntheses.[68] In 2025, the Lv group realized the free radical decarboxylative sp^3-sp^3 carbon cross-coupling reaction of GMDV with alkyl carboxylic acids through a combination of photocatalysis and palladium catalysis.[69] The photocatalytic process of the reaction (Scheme 6a) is as follows: The Ir(III) photocatalyst is excited to the excited state Ir(II)* under the irradiation of 370 nm LED; the excited state Ir(III)* oxidizes the carboxylate **L** generated by the alkyl carboxylic acid through the

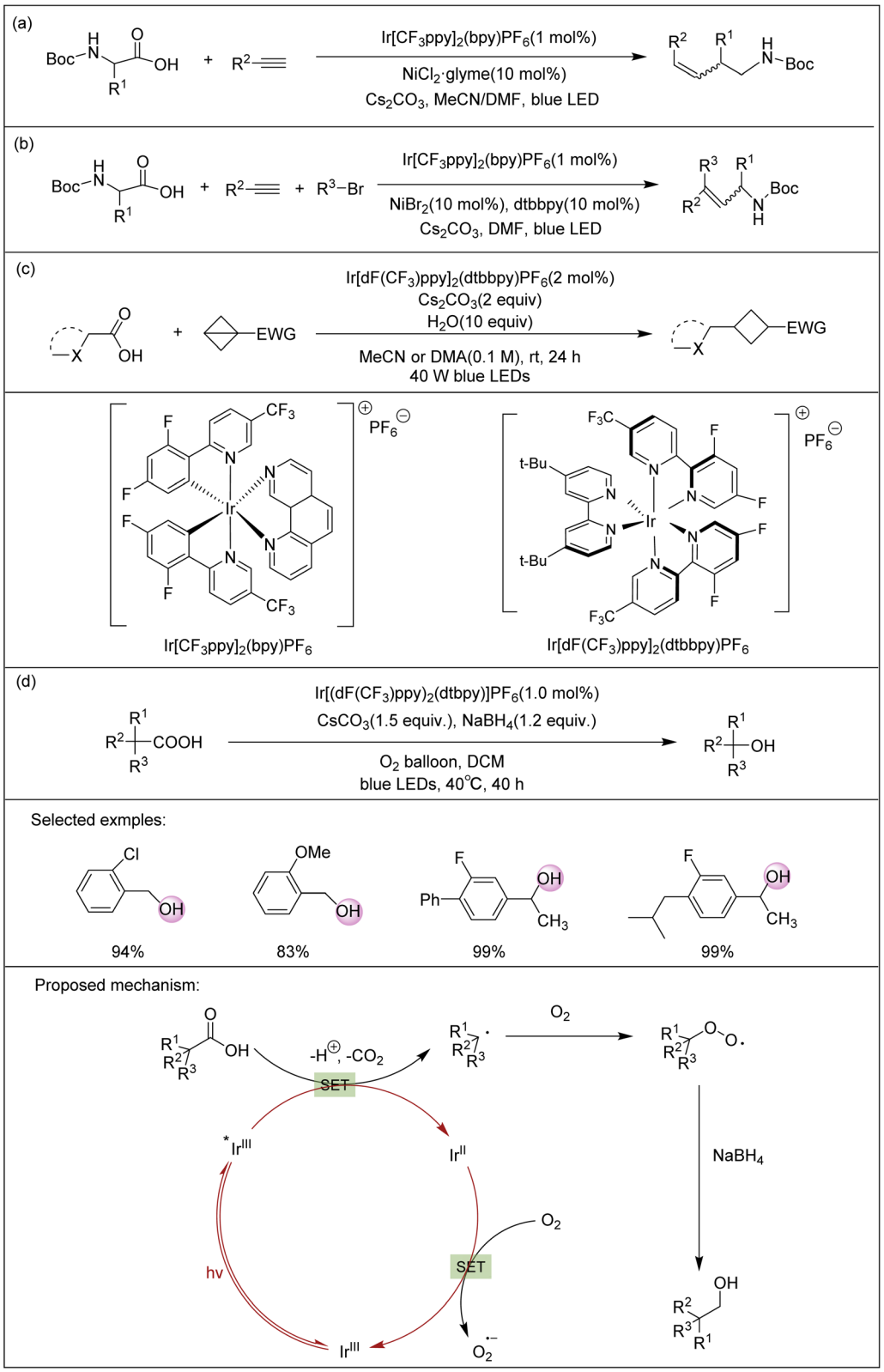

Scheme 4 (a) Photocatalytic decarboxylative addition reaction of terminal alkynes with amino acid derivatives. (b) One-pot decarboxylative three-component coupling;[62] (c) photoredox-catalyzed decarboxylative radical cyclobutylation reaction;[63] (d) photocatalytic decarboxylative oxidation reported by the Sun group. (This figure has been adapted/reproduced from ref. 65 with permission from the American Chemical Society, copyright 2020).

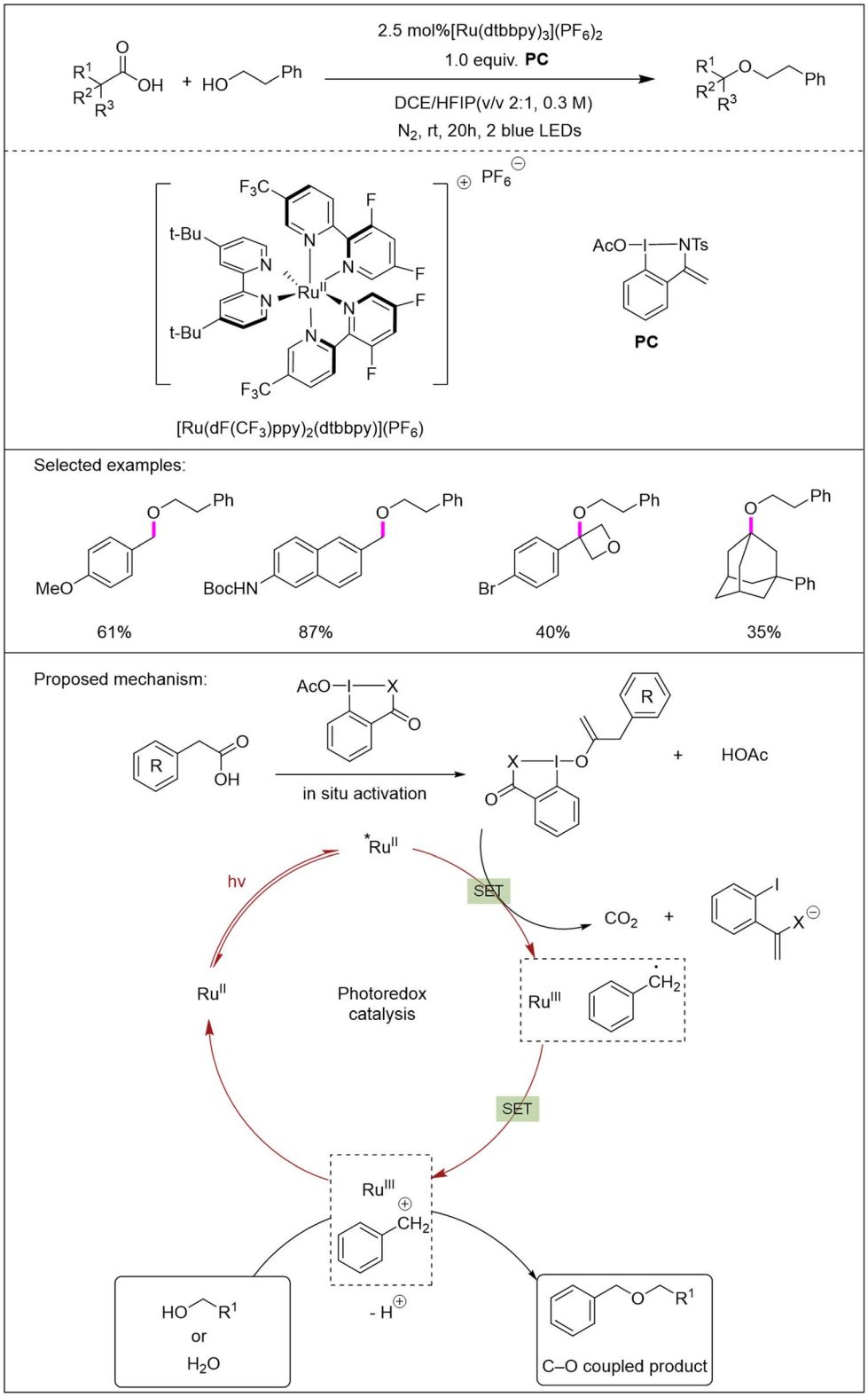

Scheme 5 Photocatalytic decarboxylative oxidation using an organic iodine photo-oxidation system reported by the Terrett group. (This figure has been adapted/reproduced from ref. 66 with permission from the American Chemical Society, copyright 2021).

SET process and is reduced to Ir(II), while carboxylate **L** is converted into the benzyl radical **K**. The generated Ir(II) undergoes a SET reaction with the Pd(I) generated in the palladium cycle. Ir(II) is oxidized back to the ground-state Ir(III) (photocatalyst regeneration), and Pd(I) is reduced back to Pd(0) (palladium catalyst regeneration), completing the entire dual catalytic

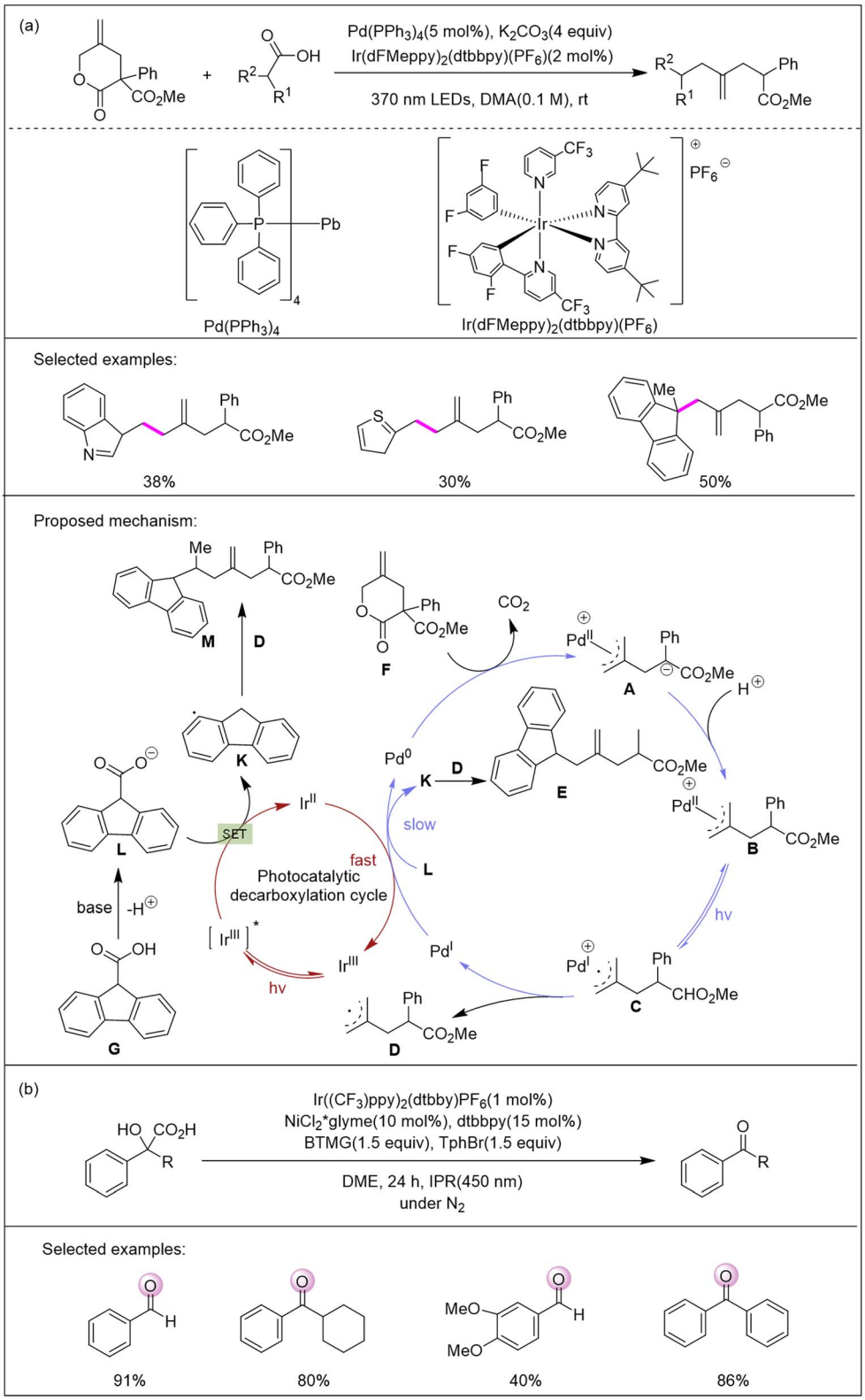

Scheme 6 (a) Free radical decarboxylative coupling of GMDV and alkyl carboxylic acids reported by the Lv group. (This figure has been adapted/reproduced from ref. 69 with permission from the Royal Society of Chemistry, copyright 2025). (b) Photocatalytic decarboxylative oxidation reaction combining nickel catalysis and photoredox catalysis.[70]

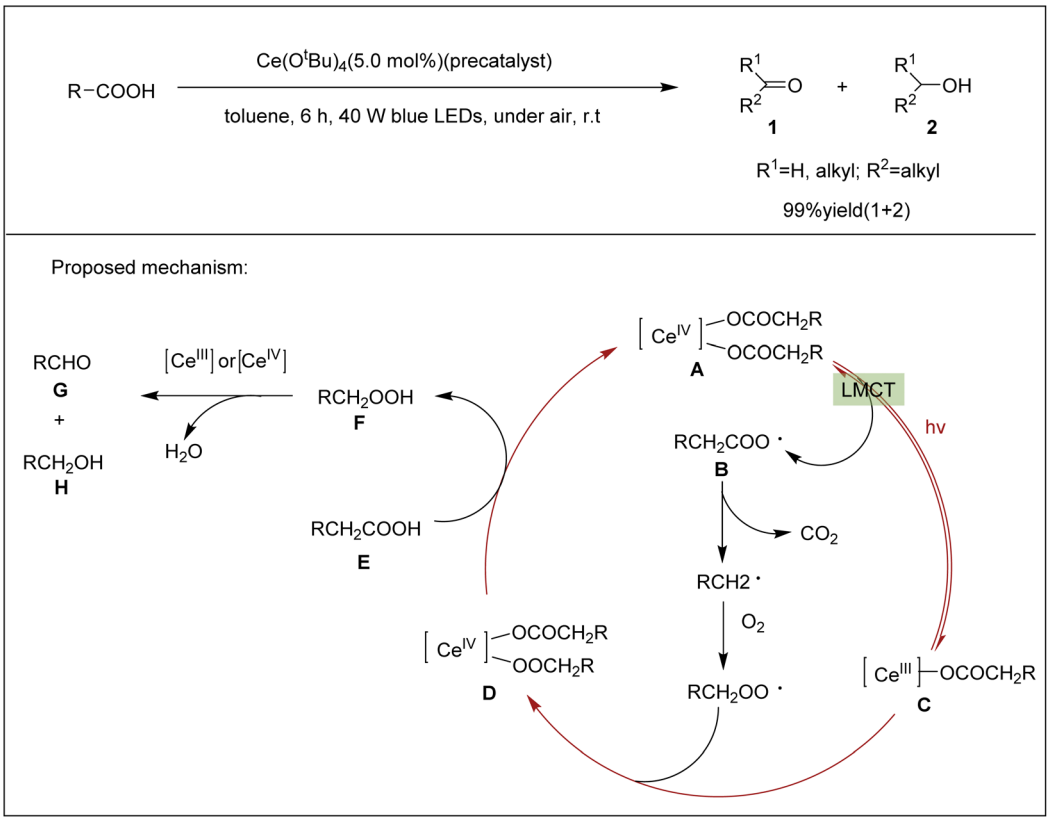

Scheme 7 Photocatalytic decarboxylative oxidation reaction of a cerium complex photocatalyst reported by the Mashima group. (This figure has been adapted/reproduced from ref. 80 with permission from the American Chemical Society, copyright 2021).

cycle. For the first time, GMDVs were used in a photocatalytic decarboxylative coupling system, which provided a mild and efficient method for C(sp^3)–C(sp^3) bond construction. The Beil group achieved the selective oxidation of α-hydroxy acids (especially mandelic acid) by combining nickel catalysis and photoredox catalysis, which can efficiently produce aldehydes and ketones without peroxidation.[70] This method proceeds efficiently under radical conditions *via* decoupled decarboxylation and alcohol oxidation steps, and it was further extended to the decarboxylative oxidation of β-hydroxy acids and phenylglycine, affording carbonyl compounds upon hydrolysis (Scheme 6b).

3. Simple transition metal salt photocatalysts

The simple transition metal salt catalyst for photocatalytic decarboxylation mainly excites the metal center through the LMCT process to generate the free radical intermediates of carboxylic acid derivatives, thereby achieving decarboxylation. Typical catalysts include iron salts, copper salts, and cerium–zirconium-manganese mixed metal clusters.[71–73] These metal salts can efficiently promote the decarboxylation, nitridation, halogenation, and oxidation of carboxylic acids under visible light irradiation. The advantages of these simple transition metal salt catalysts are their low cost, simple operation, environmental friendliness, and good functional group compatibility. At the same time, the synthesis and use of complex ligands are avoided, and the system complexity and risk of by-product formation are reduced.[74–76]

The unique reactivity of Ce(OAc)$_4$, a highly oxidized metal acetate, can easily produce reactive carboxyl radicals under light irradiation, which can be carried out with only a catalytic amount. The continuous homolysis of the covalent bonds of Ce(IV)–ligands produces synthetically useful organic radicals, which are used for the formation of various C–C, C–N and C–O bonds. At the same time, the electronic transition of Ce(III), *i.e.*, 4f → 5d excitation, produces the excited Ce(III) species as a strong reducing agent. In these Ce(III) photocatalysts, since the energy level of the 5d orbital is very sensitive to the supporting ligand, the emission properties of 5d → 4f can be controlled by the molecular design of the ligand.[77–79] In 2021, the Mashima group studied the photocatalytic carboxylate decarboxylation oxidation strategy of Ce(IV).[80] The carboxylate Ce(IV) complex, spontaneously formed from the precursor Ce(OtBu)$_4$ and the corresponding carboxylic acid in toluene, acts as an effective photocatalyst for the decarboxylation of aliphatic carboxylic acids. This complex catalyzes aliphatic carboxylic acids to form C–O bond products, including aldehydes, ketones, and alcohols. Based on the experimental results and relevant literature reports, a plausible reaction mechanism is proposed (Scheme 7): Ce(OtBu)$_4$ reacts with the substrate

carboxylic acid to form a hexanuclear carboxylic acid Ce(IV) carboxylate **A**, which is then photolyzed to form the corresponding carboxyl radical **B**, and Ce(IV) species **A** is reduced to Ce(III) species **C**. Because the carboxyl radical is very unstable, it readily undergoes spontaneous decarboxylation to obtain the corresponding alkyl radical, which easily reacts with oxygen to form an alkyl peroxide radical. Subsequently, the peroxyl radical oxidizes Ce(III) to obtain peroxidized Ce(IV) alkyl **D**. The exchange of ligands with carboxylic acid **E** leads to the regeneration of carboxylic acid Ce(IV) and the release of alkyl hydroperoxide **F**. The alkyl hydroperoxides in the reaction mixture are decomposed by Ce(III) and Ce(IV) to obtain the corresponding aldehydes **G** and alcohols **H**, respectively. The reaction features a broad substrate scope and notable functional group tolerance: beyond various aliphatic carboxylic acids, *ortho*-, *meta*-, and *para*-substituted arylacetic acids with different electronic properties (*e.g.*, halogenated, methoxylated derivatives) are also compatible with this reaction.

In 2023, for the first time, the West group combined an iron catalyst (Fe^{3+}) with a thiol derivative (TRIP disulfide) to achieve decarboxylative protonation.[81] Although iron has been shown to catalyze decarboxylation, most of these reactions are thermally driven and require activated carboxylic acids and strong stoichiometric oxidants. This reaction requires no substrate preactivation or noble metal photocatalysts (*e.g.*, Ir/Ru); it only uses earth-abundant iron to overcome the limitation of substrate compatibility. The author proposes that the mechanism of the reaction goes through the inner LMCT process, which can avoid the non-selective outer electron transfer of the electron-rich functional groups in the SET process, thereby significantly expanding the substrate range of the hydrodecarboxylation. Thus, the substrate that is incompatible with the acridinium method can participate in the reaction. In addition, the covalent pre-binding of the substrate to the iron photocatalyst avoids the lifetime limitation of the excited state caused by the excitation-dependent molecular bimolecular reaction in the outer electron transfer method (Scheme 8). Deprotonated carboxylate anions and Fe^{3+} form complex **A**; **A** becomes an excited state **B** under light irradiation, and then **B** generates Fe^{2+} **C** and **D** through the LMCT process. At the same time, TRIP

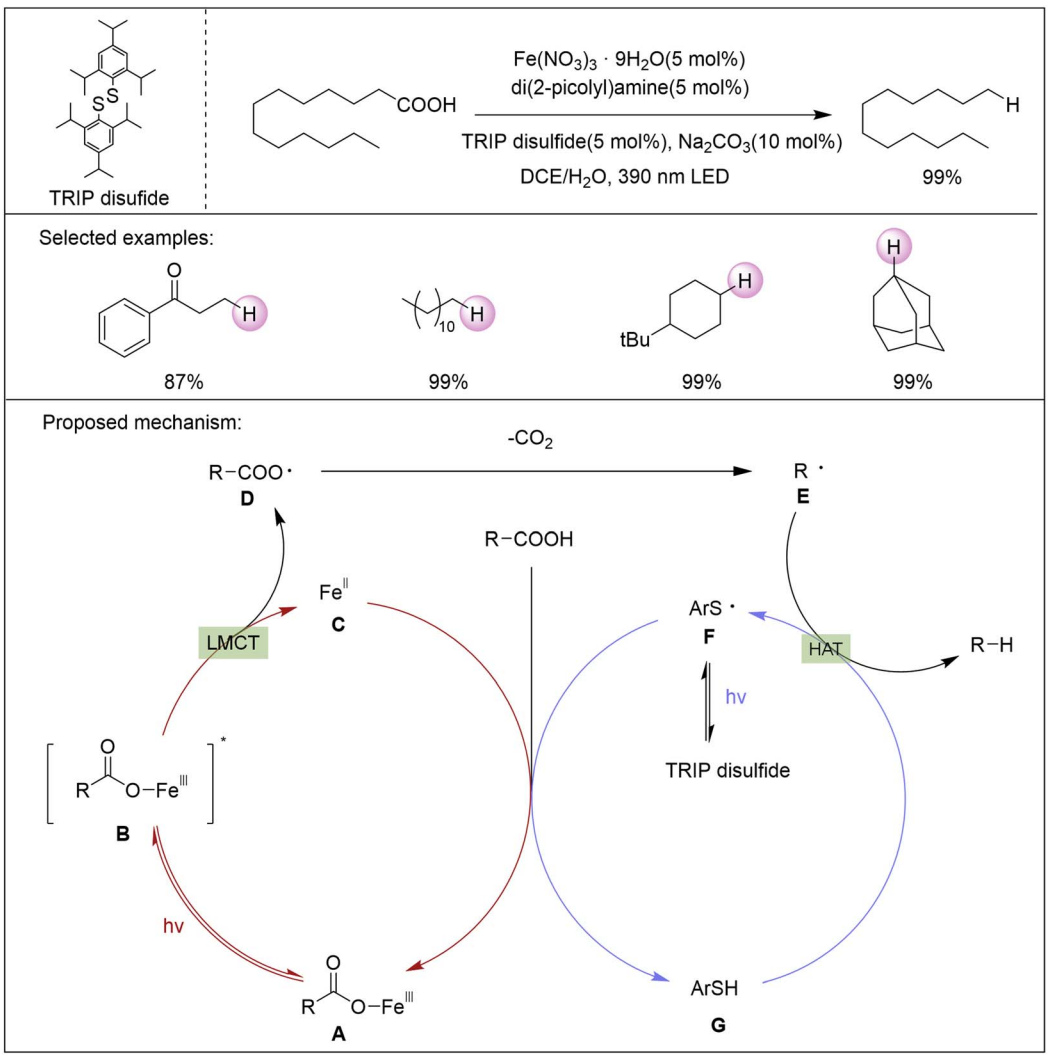

Scheme 8 Photoinduced iron/thiol dual-catalyzed decarboxylative protonation. (This figure has been adapted/reproduced from ref. 81 with permission from Springer Nature, copyright 2023).

disulfide is homolytic to form free radical **F**; **F** captures the electrons in **C** and the proton-generating substance **G** in the acid, and **G** finally generates the final reduction product through the HAT process. It is worth noting that the use of this condition can make the dicarboxylic acid substrate undergo double decarboxylation to obtain 82% of the product. The authors also examined the applicability of a variety of complex natural products and drugs. For example, the reaction of loxoprofen at the gram scale can produce 82% of the product overnight. In the same year, the team also used $Fe(NO_3)_3 \cdot 9H_2O$ as a dual-use catalyst and oxidant to directly convert a variety of challenging inactivated primary, secondary and tertiary substrates into organic azides under visible light irradiation conditions.[82] They demonstrated that nitrate acts as an essential terminal oxidant against anions, thereby eliminating the need for external chemical oxidants and solving the long-term problem of catalyst turnover in the LMCT/RPC process. In addition, they elucidated the mechanism by which LMCT initiates decarboxylation to generate alkyl radicals, which then inhibit unnecessary elimination and rearrangement pathways through RLT rather than RPC.

In 2025, the Li group developed an iron-catalyzed decarboxylative alkynylation reaction, enabling the efficient coupling of carboxylic acids with alkynyl bromides.[83] With commercially available $Fe(OTf)_3$ (5 mol%) as the catalyst, under 390 nm visible light irradiation at room temperature and with Cs_2CO_3 as the base, high-yielding decarboxylative alkynylation products are obtained in a CH_3CN solvent. The reaction is compatible with structurally diverse carboxylic acids, including α-amino acids, dipeptides, aliphatic acids, and complex medicinal acids. Based on the mechanism verification, the reaction mechanism conforms to the general LMCT process (Scheme 9). In the same year, the Tsurugi group proposed the introduction of light-responsive Ce(IV) centers into photochemically stable Zr/Hf oxygen/hydroxyl bridged clusters.[84] Through metal-to-metal substitution, a single cerium-doped six-core mixed metal cluster ($CeZr_5$ core) is formed. UV-vis spectroscopy and DFT calculations show that the introduction of Ce(IV) affects the HOMO–LUMO energy gap, making the cluster absorb in the visible region, and that the introduction of manganese increases the electron density of the cluster. Using Ce–Zr bimetallic synergistic catalysis, a variety of carboxylic acids were converted into alcohols with one less carbon atom in an air atmosphere, and the yield was excellent.

4. Metal-free homogeneous photocatalysts

The metal-free photocatalyst completely avoids metal, and the reaction conditions are extremely mild. Thus, the reaction can be applied to the post-modification of polypeptides and drug molecules (such as aspirin and penicillin derivatives) without destroying the existing complex structures in the molecules. Such catalysts usually induce carboxylic acid derivatives to generate free radical intermediates through the SET process or energy transfer mechanism generated by photoexcitation; they mainly include acridine and 4CzIPN.[85–87] In addition, some organic dyes, such as fluorescein dimethylammonium, have been shown to achieve the decarboxylative acylation of pyridine *N*-oxides at room temperature.[88] Conjugated aromatic hydrocarbon materials represented by covalent triazine framework (CTF-2) can be used as solid-state photocatalysts to achieve decarboxylative addition reactions with good recyclability and stability.[89] Such catalysts have diverse structures and can easily regulate their electronic properties. They can efficiently absorb visible light and participate in reversible redox processes, thereby driving the reaction. However, the catalytic efficiency is limited by their absorption of visible light and the lifetime of the excited state, resulting in unstable reaction efficiency. Second, organic dyes are prone to photodegradation or structural damage during repeated use, affecting the stability and recycling of the catalyst, thereby increasing the cost and difficulty of waste treatment. Although the metal-free advantage is obvious, the synthesis of some organic dyes is complex and costly, which is not conducive to large-scale industrial applications. Therefore, improving the stability, selectivity and economy of organic dyes and conjugated aromatic photocatalysts is still an important challenge in current research.[90–93]

The Nicewicz group developed an acridinium photocatalytic system with Mes-Acr-Ph as the photosensitizer and $(PhS)_2$ as the cocatalyst, enabling the efficient hydrodecarboxylation of diverse carboxylic acids.[94] However, this reaction requires expensive trifluoroethanol (TFE) as a solvent, and the yield of this reaction for long-chain fatty acids is only 49%. The reaction produces carbon radicals through the SET process. In the presence of electron-rich aromatics, this competitive outer electron-transfer process leads to the low efficiency of the formation of key carboxyl radicals required for decarboxylation. In 2018, the Sun group reported the decarboxylative alkylation tandem nitrile insertion/cyclization reaction of alkyl carboxylic acids with aryl acrylamide derivatives.[95] The authors ingeniously combined an organic dye (eosin Y) with $(NH_4)_2S_2O_8$ to achieve the decarboxylative radical reaction of alkyl carboxylic acids, enabling subsequent nitrile insertion and cyclization to afford alkyl phenanthridine compounds (Scheme 10a). The reaction involves imine nitrogen radical intermediates. Except for pivalic acid, primary carboxylic acids (isovaleric acid, 2-cyclohexylacetic acid) and cyclic secondary carboxylic acids can be smoothly coupled with *N*-arylacrylamide to obtain addition/cyclization products in good yields. In 2018, the Aggarwal group achieved the direct synthesis of cyclopropanes from carboxylic acids and chlorinated olefins *via* a photocatalytic decarboxylative radical addition-polar cyclization cascade reaction.[96] The authors propose that alkyl carboxylic acids and electron-deficient olefins can be converted into carbanion intermediates *via* radical polarity reversal during reduction; these intermediates then undergo intramolecular alkylation with alkyl chlorides to afford cyclopropane compounds (Scheme 10b). This reaction system is compatible with various alkyl carboxylic acids and haloalkyl olefins as substrates, providing a highly atom-economical synthetic route for preparing diverse cyclopropane compounds.

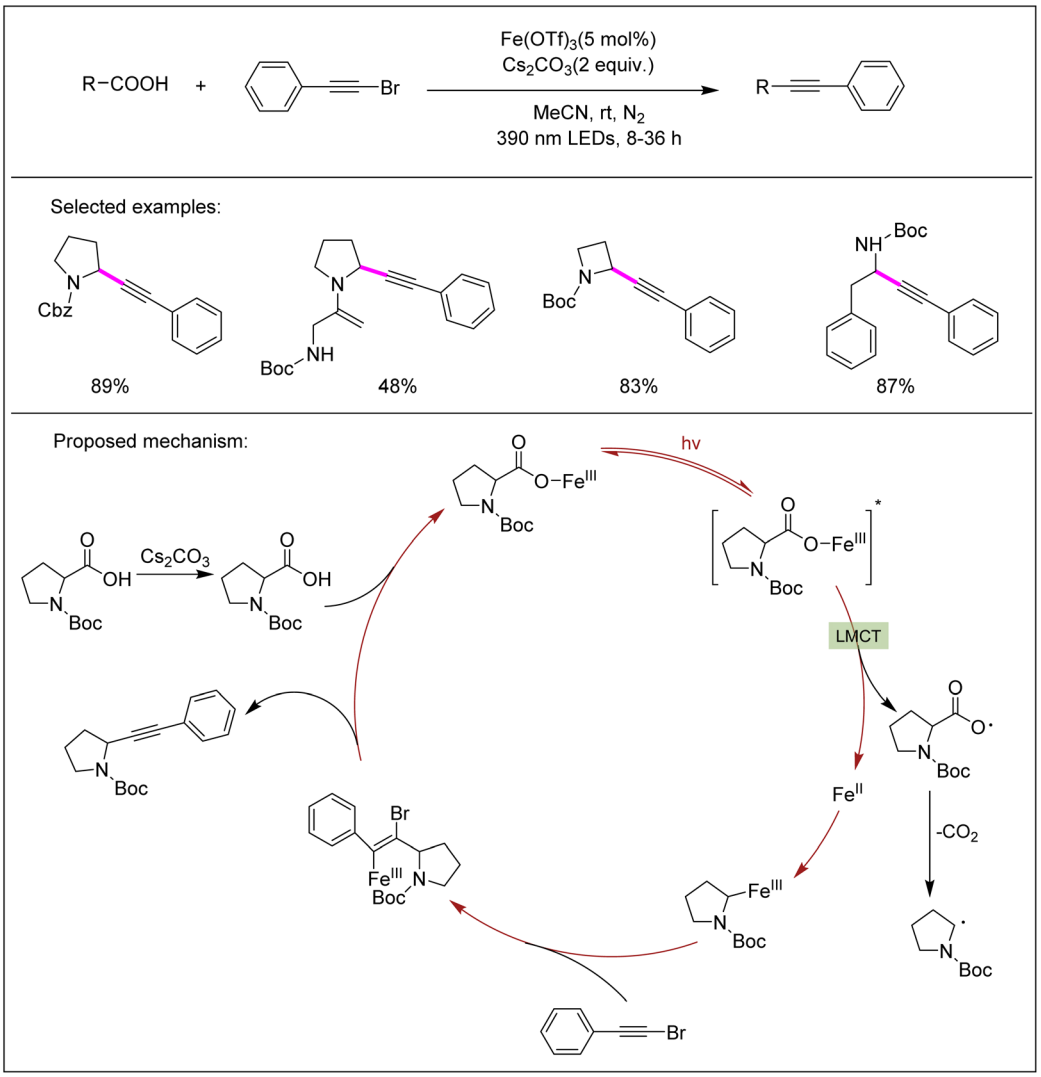

Scheme 9 $Fe(OTf)_3$-catalyzed decarboxylative alkynylation reaction reported by the Li group. (This figure has been adapted/reproduced from ref. 83 with permission from the American Chemical Society, copyright 2025).

In 2020, the Mastandrea and his co-workers reported an innovative cooperative copper-photoredox dual catalytic system, enabling the decarboxylative hydroalkylation of heteroaromatic terminal alkynes with carboxylic acids. Notably, the Z/E stereochemistry of the products can be switched by adjusting the combination of the ligand and base, and it is applicable to the stereoselective coupling of primary, secondary, and tertiary alkyl radicals (generated from carboxylic acids) with alkynes.[97] This mechanism was proposed by the author (Scheme 11). Under light irradiation, the photocatalyst (4CzIPN) attains its excited state (PC*) and can both reduce Cu(II) complexes in the solution and oxidize α-amino and α-oxy carboxylates. The Cu(I) complex generated either through the disproportionation of the Cu(II) source or the SET process from PC* can form complex **A** (which may exist as a monomer, polymer, or both) with the aid of a base (CsOAc). The direct photoexcitation of **A** to **A*** could induce charge depletion on the alkyne moiety *via* the LMCT process, thereby accelerating the attack by radical **E** (formed through the deprotonation and single-electron oxidation of **D**, possibly mediated by PC*). This addition leads to the formation of vinyl radical **B**, which then reacts to form the corresponding vinyl anion **C** while oxidizing $PC^{\bullet-}$. Subsequent protonation of the anion and proto-demetallation of the Cu–C bond yield the target product. This dual catalytic system activates alkynes through the LMCT process of copper–acetylene complexes and couples with photoredox catalysis to generate alkyl radicals, thereby surmounting the kinetic barriers associated with alkyne radical addition. The method is compatible with a wide range of alkyl carboxylic acids (including those containing α-heteroatoms) and hetero aryl alkynes and has been extended to the C–H vinylation of aromatic amines.

In 2020, The Mega and colleagues achieved the first decarboxylative coupling of vinyl borates through a nickel/photoredox dual catalytic strategy, achieving three-component efficient coupling,[98] overcoming the secondary alkyl radical side-reaction problem and expanding the application of α-

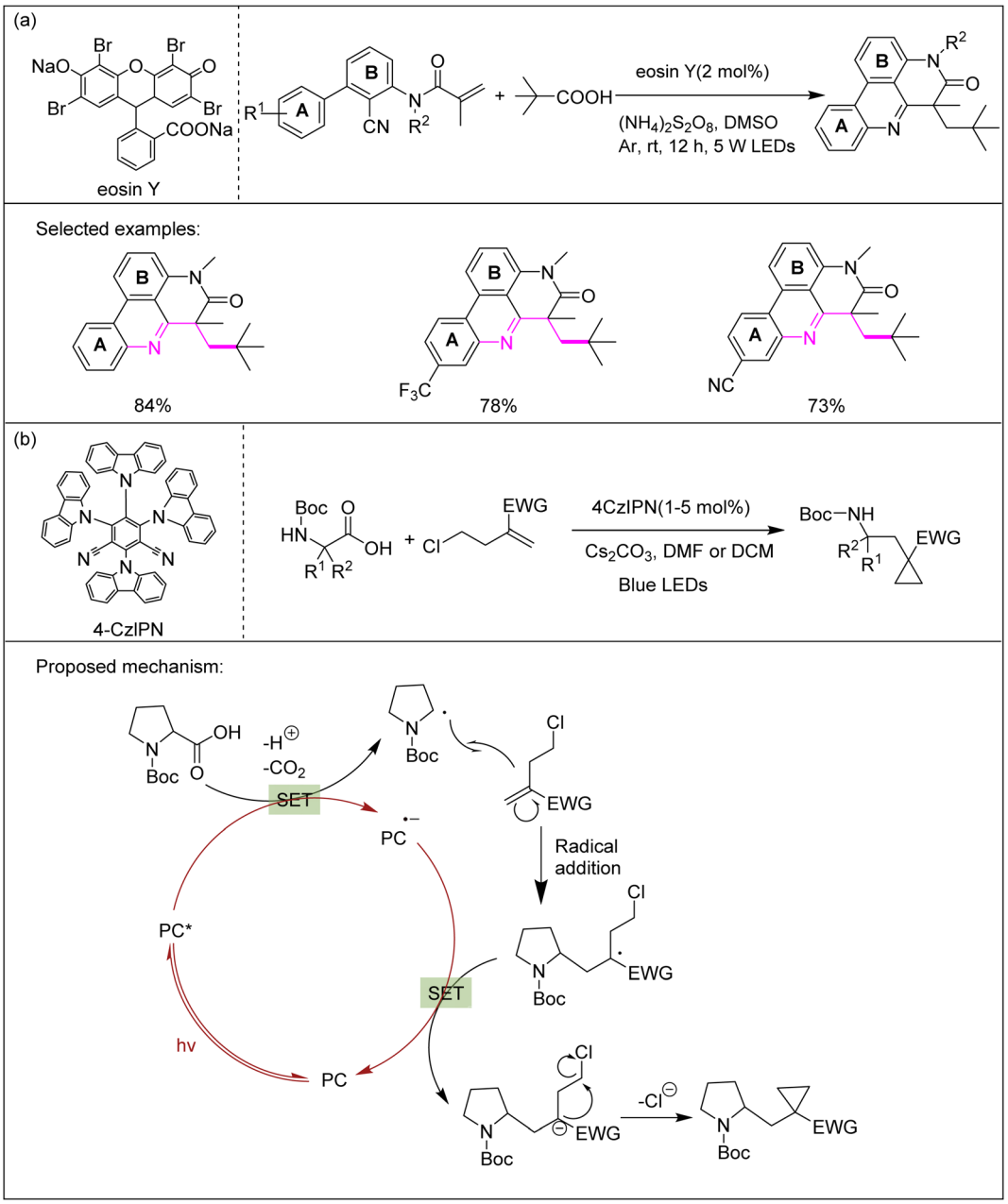

Scheme 10 (a) Decarboxylation method involving the combination of eosin Y and $(NH_4)_2S_2O_8$ reported by the Sun group.[95] (b) Decarboxylative radical addition-polar cyclization tandem reaction using the 4CzIPN photocatalyst. (This figure has been adapted/reproduced from ref. 96 with permission from Wiley, copyright 2018).

amino acids in coupling reactions. The author proposes the following mechanism (Scheme 12): the photocatalyst PC (4CzIPN) is excited by blue light to form PC*; PC* and **A** undergo a SET process to form a carboxylic acid radical. The carboxylic acid radical quickly removes CO_2 to form an alkyl radical **B**. The alkyl radical **B** is added to the double bond of the vinyl borate **C** to form an α-boryl radical **D**. The stabilizing effect of the α-boryl free boron is more stable than that of ordinary alkyl radicals and inhibits side reactions. At the same time, the Ni catalyst is oxidized to aryl iodide to form an aryl Ni(II) complex. The α-boryl radical **D** is captured by the aryl Ni(II) complex to form the Ni(III) intermediate **E**. Finally, the Ni(III) intermediate is reduced and eliminated to form the three-component coupling product **F** and Ni(I) species. The reduced state ($PC^{\bullet-}$) of the photocatalyst oxidizes the Ni(I) species to Ni(0) and completes the nickel catalytic cycle. At the same time, $PC^{\bullet-}$ is oxidized to PC and completes the photocatalytic cycle.

In 2022, the Sun and colleagues achieved the decarboxylation of C10–C18 fatty acids with a yield of up to 98% using a methoxy-substituted mediator and 4,4′-dimethyldiphenyl disulfide as the HAT reagent, with low-cost ethyl acetate as the solvent.[99] At the same time, heavy water (D_2O) was used as the

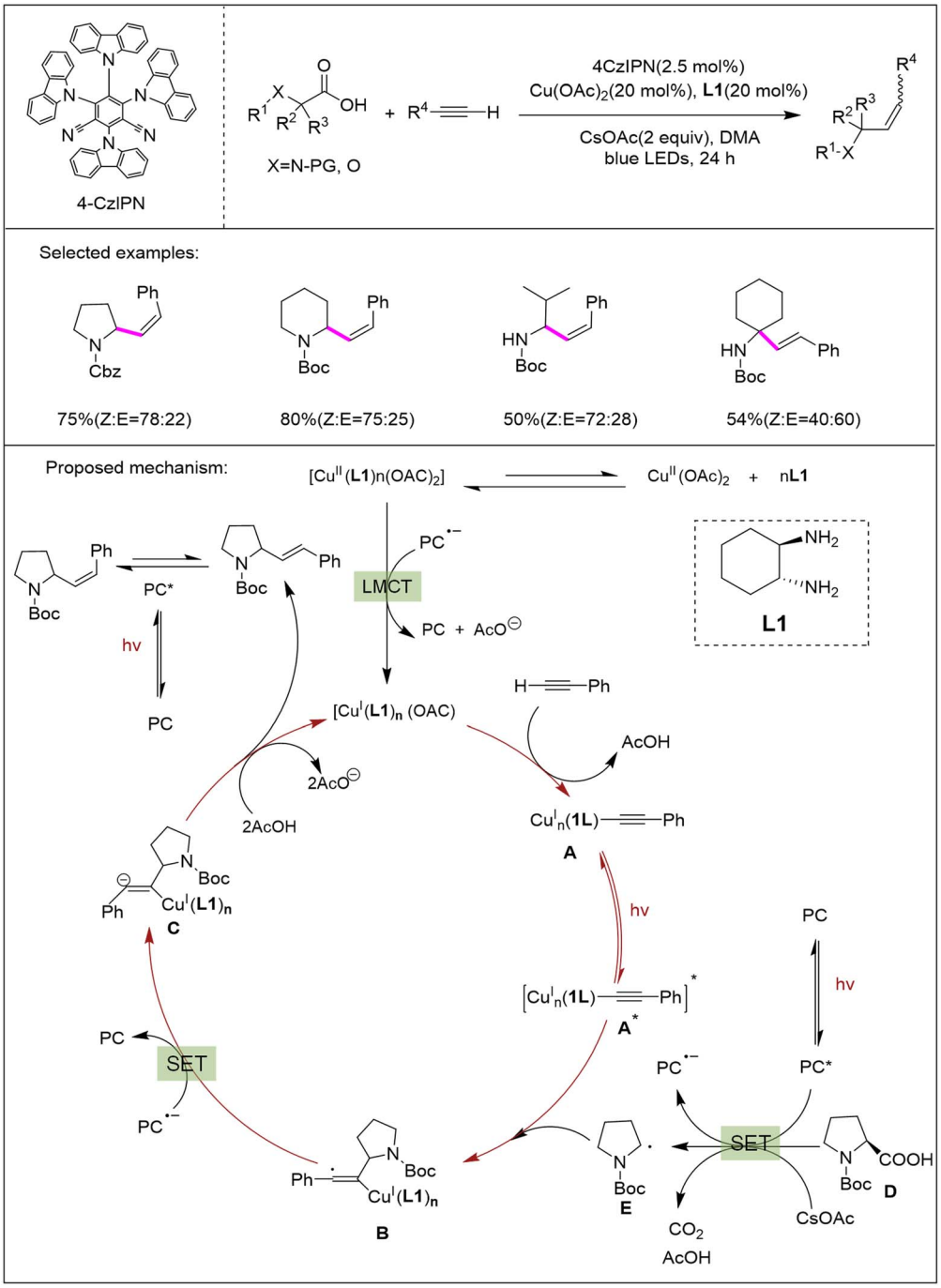

Scheme 11 Photoredox/copper-catalyzed decarboxylative alkylation of alkynes. (This figure has been adapted/reproduced from ref. 97 with permission from the American Chemical Society, copyright 2020).

deuterium source to achieve an efficient decarboxylative deuteration reaction. Through a variety of experimental verification processes, the following mechanism is proposed (Scheme 13). Photocatalyst **A** changed from ground state to excited-state **B** under visible light irradiation. B exhibits strong oxidizability. The electron of deprotonated **C** was captured by the SET process to generate **D**, and then **D** quickly removed CO_2 to generate alkyl radical **J**. At the same time, disulfide **F** was homolyzed under light irradiation to generate free radical **G**. **G** rapidly captured the electrons in catalyst **E** to generate thiophenol anion **H**. **H** obtained protons in acid to generate **I**. The final product is obtained *via* the hydrogen atom transfer process. This synergistic mechanism may effectively inhibit competitive side reactions by quenching active alkyl radicals.

In 2022, the Kim and colleagues reported a visible light-mediated photocatalytic decarboxylative pyridine reaction.[100] The C4-selective C–H alkylation of carboxylic acids with *N*-amido pyridinium salts has been achieved utilizing *in situ*-

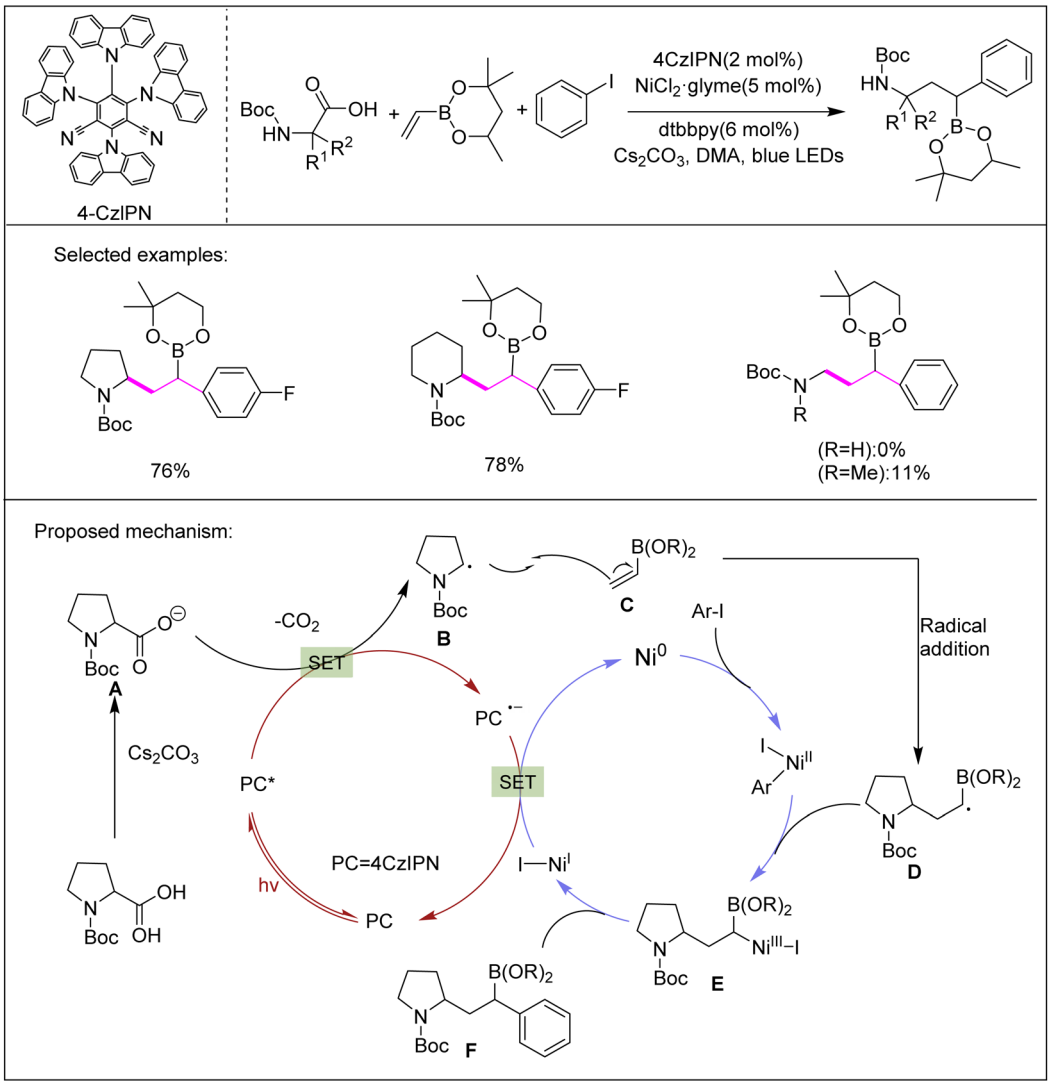

Scheme 12 Three-component decarboxylative coupling catalyzed by metal photoredox reported by the Mega. (This figure has been adapted/reproduced from ref. 98 with permission from Wiley, copyright 2020).

generated amide radicals as oxidants without the need for external oxidants or metals. This protocol addresses key limitations of traditional Minisci-type reactions, including the requirement for strong acids, excessive use of carboxylic acids, generation of toxic waste, and poor selectivity. The radical mechanism was confirmed *via* radical trapping experiments and Stern–Volmer quenching studies (Scheme 14a): under alkaline conditions, the carboxylic acid first deprotonates to form carboxylate **D**. At the same time, photocatalyst **A** is excited to the excited-state **B** under blue light irradiation. The excited photocatalyst oxidizes carboxylate *via* the SET process to generate a carboxyl radical and reduced photocatalyst **C**. The carboxyl radical rapidly releases CO_2 to generate a highly active alkyl radical. The generated alkyl radical selectively attacks the C4 position **F** of an *N*-amido pyridinium salt (*N*-amido substitution endows the pyridinium salt with inherent C4 reactivity, avoiding the C2/C4 selectivity problem of traditional Minisci reactions), forming pyridyl-alkyl addition intermediate **G**. This step is key to achieving "C4 selectivity" in the reaction. Intermediate **G** was deprotonated first, then decomposed by N–N bond homolytic cleavage to generate the target product **I** and the *in situ*-generated amide radical **H**. **H** exhibits strong oxidation ability. The excited-state **C** was regenerated into the ground-state photocatalyst **A** through the SET process, and it was converted into a stable amine product. This step does not require an external oxidant. Reverse glycosyl fluoride (RGF) is a fluorinated sugar with a special structure; it is the key intermediate of many drugs (such as anti-hepatitis B drug precursors and anti-tumor drugs). Because the carboxylate anion of uronic acid is difficult to oxidize, it is difficult to synthesize nucleosides with this specific stereo configuration by traditional ion reactions. The oxidation potential of the commonly used Ir complex $Ir[dF(CF_3)ppy]_2(dtbbpy)PF_6$ is about 1.69 V (*vs.* SCE), and the oxidation potential of riboflavin (vitamin B2 derivative) is about 1.50 V (*vs.* SCE). In 2022, RGF was synthesized using 9-methylthio-10-methylacylperchlorate (Mes-Acr ClO_4) as

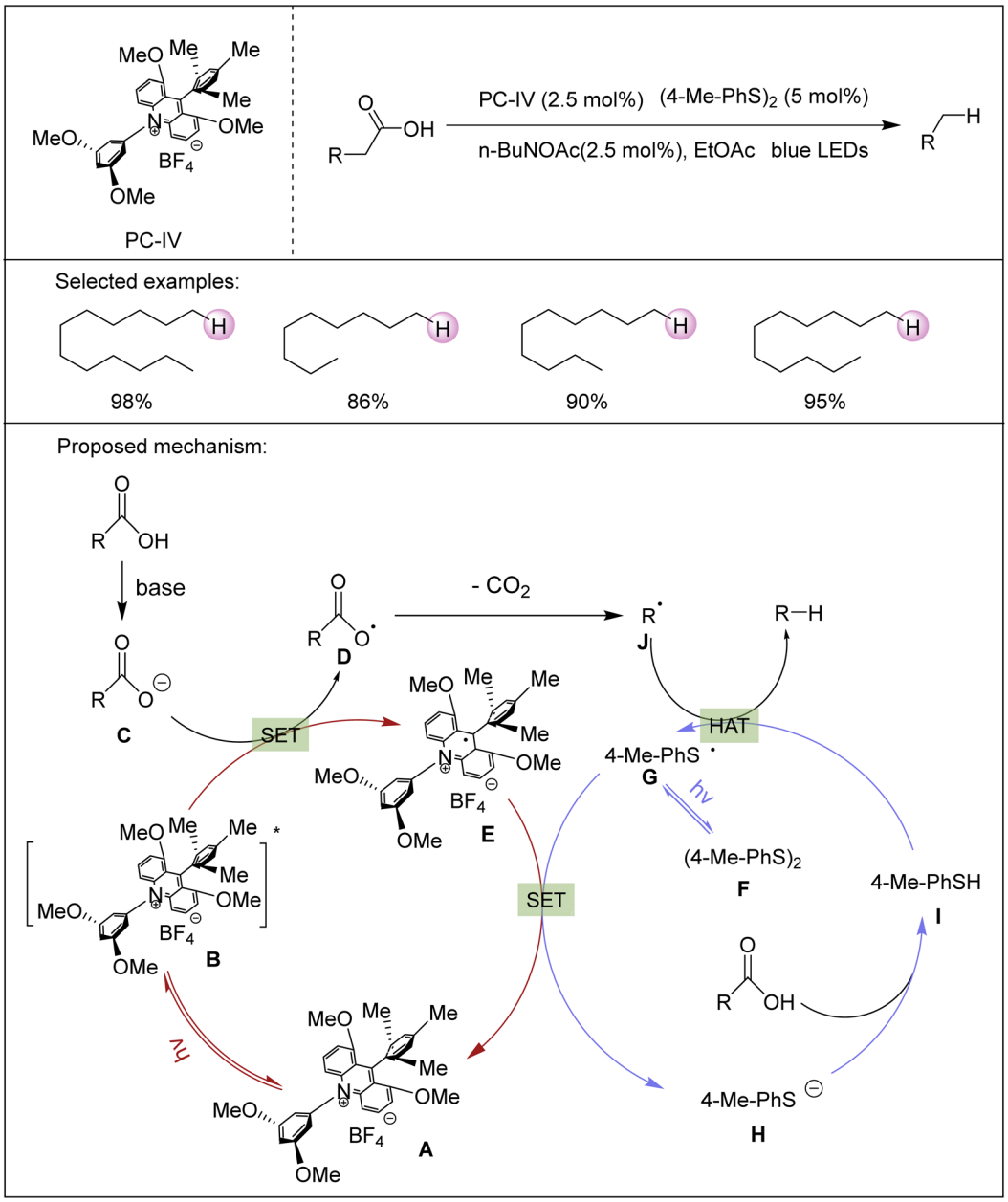

Scheme 13 Hydrodecarboxylation using a methoxy-substituted acridine photocatalyst. (This figure has been adapted/reproduced from ref. 99 with permission from Wiley, copyright 2022).

a photocatalyst with its high excited oxidation-state potential (2.06 V *vs.* SCE).[101] The reaction showed good adaptability to both furanuronic and pyranuronic acids. RGFs containing tertiary carbon–fluorine bonds and disaccharide-derived RGFs were successfully synthesized. It is especially suitable for the uronic acid of D-ribose and L-lyxose configurations and can also enable the efficient preparation of rare L-lyxose-configuration RGF nucleosides (Scheme 14b).

Tetraalkyl-substituted pyridine photoredox catalysts (PPTs) are effective organic photocatalysts with strong excited-state oxidation ability ($E^*_{red} = +2.10$ V *vs.* SCE in MeCN). These catalysts can be synthesized *via* photo-mediated oxygen atom transfer from their *n*-oxide precursors and exhibit a three-state excited state.[102] As dual-photoredox catalysts and hydrogen atom transfer catalysts, they can achieve a variety of transformations, such as the hydroacetoxylation of activated olefins, hydroamination of styrene and primary amines, and decarboxylation of electron-deficient olefins. Tetraazasubstitution improves their catalytic activity and stability, allowing efficient single-electron oxidation processes under mild conditions without the need for metals.[103–105] In 2022, the Mayer and colleagues used an organic pyrimidine–pteridine photoredox catalyst for different primary, secondary, and tertiary carboxylic acids.[106] The reaction conditions were optimized *via* statistical experimental design (DoE). This work achieved the use of commercially available tablets of non-steroidal anti-

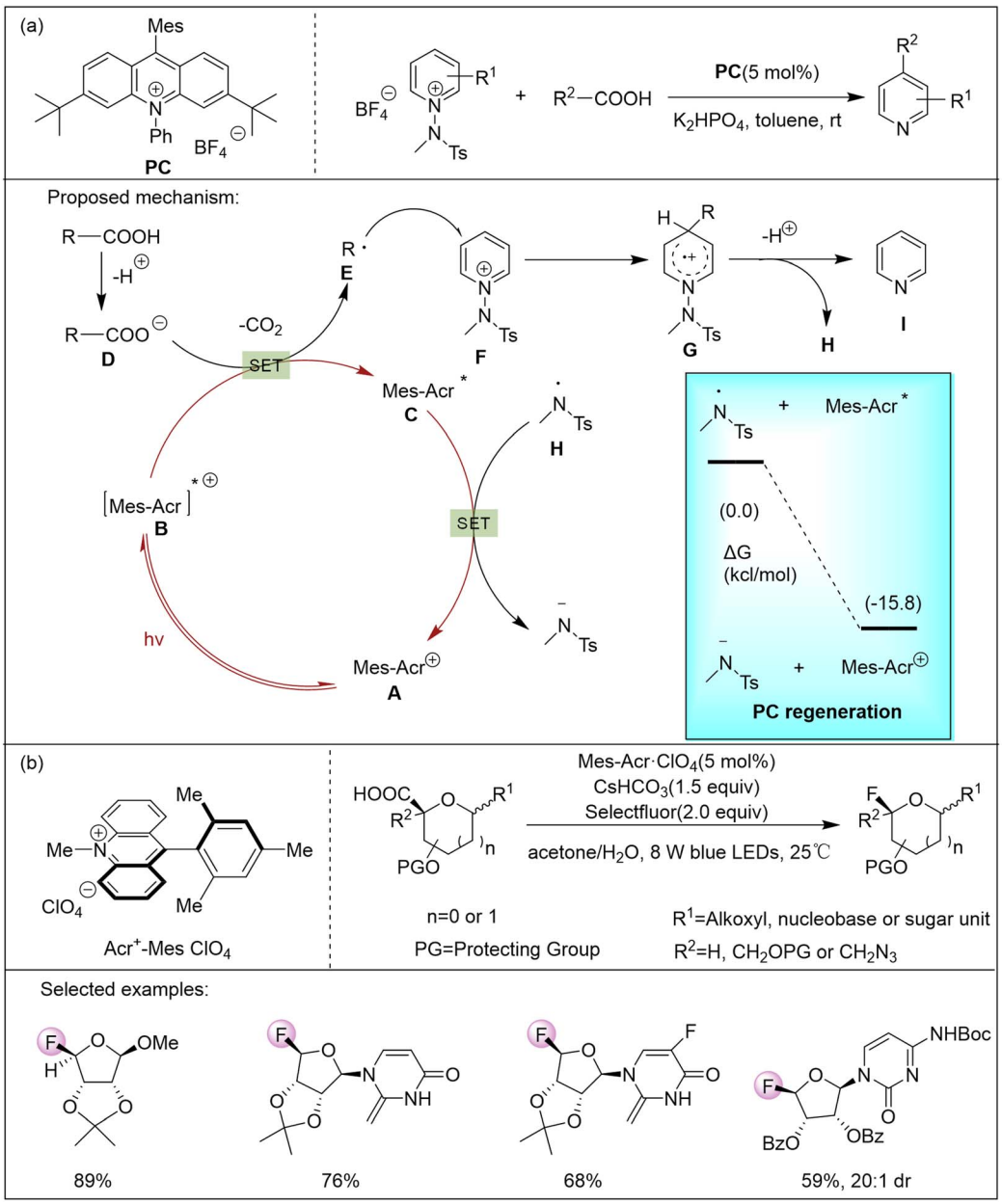

Scheme 14 (a) C4-selective decarboxylative alkylation of heteroarenes reported by the Kim and colleagues. (This figure has been adapted/reproduced from ref. 100 with permission from the American Chemical Society, copyright 2022). (b) Photocatalytic decarboxylative fluorination reaction reported by the Li group.[101]

inflammatory drugs (NSAIDs) and gram-scale conversion. The reaction mechanism was discussed through experiments (Scheme 15). Carboxylic acids **E** undergo deprotonation with K_3PO_4 to form aliphatic carboxylates **F**. These carboxylates then undergo oxidative decarboxylation under the mediation of photoexcited PrPPT* **B**, producing alkyl radicals G and the radical anion catalyst $PrPPT^{\bullet -}$ **C**. Next, $PrPPT^{\bullet -}$ **C** accepts a proton from another carboxylic acid molecule to form $PrPPTH^{\bullet}$ **D**. Finally, $PrPPTH^{\bullet}$ **D** carries out hydrogen atom transfer to alkyl radicals **G**; alkane products **H** are formed, and the photocatalyst is regenerated. The reaction substrates cover a variety of biologically active aliphatic carboxylic acids. When D_2O is used as a cheap deuterium source, the deuteration rate can reach up to 95%.

In 2024, the Zhang and colleagues proposed the use of simple aliphatic ketones (diacetyl) as a photocatalyst to replace expensive metal complexes and complex organic dyes to directly decarboxylate fluorinated aliphatic carboxylic acids and diacids.[107] Decarboxylative fluorination is preferred over C(sp^3)–H, which is common in ketone catalysts, because the decarboxylative SET kinetic rate is significantly faster than the HAT rate. The oxidation ability of the ketone radical cation determines the scope of application of the carboxylic acid substrate, and its oxidation potential needs to be higher than that of the

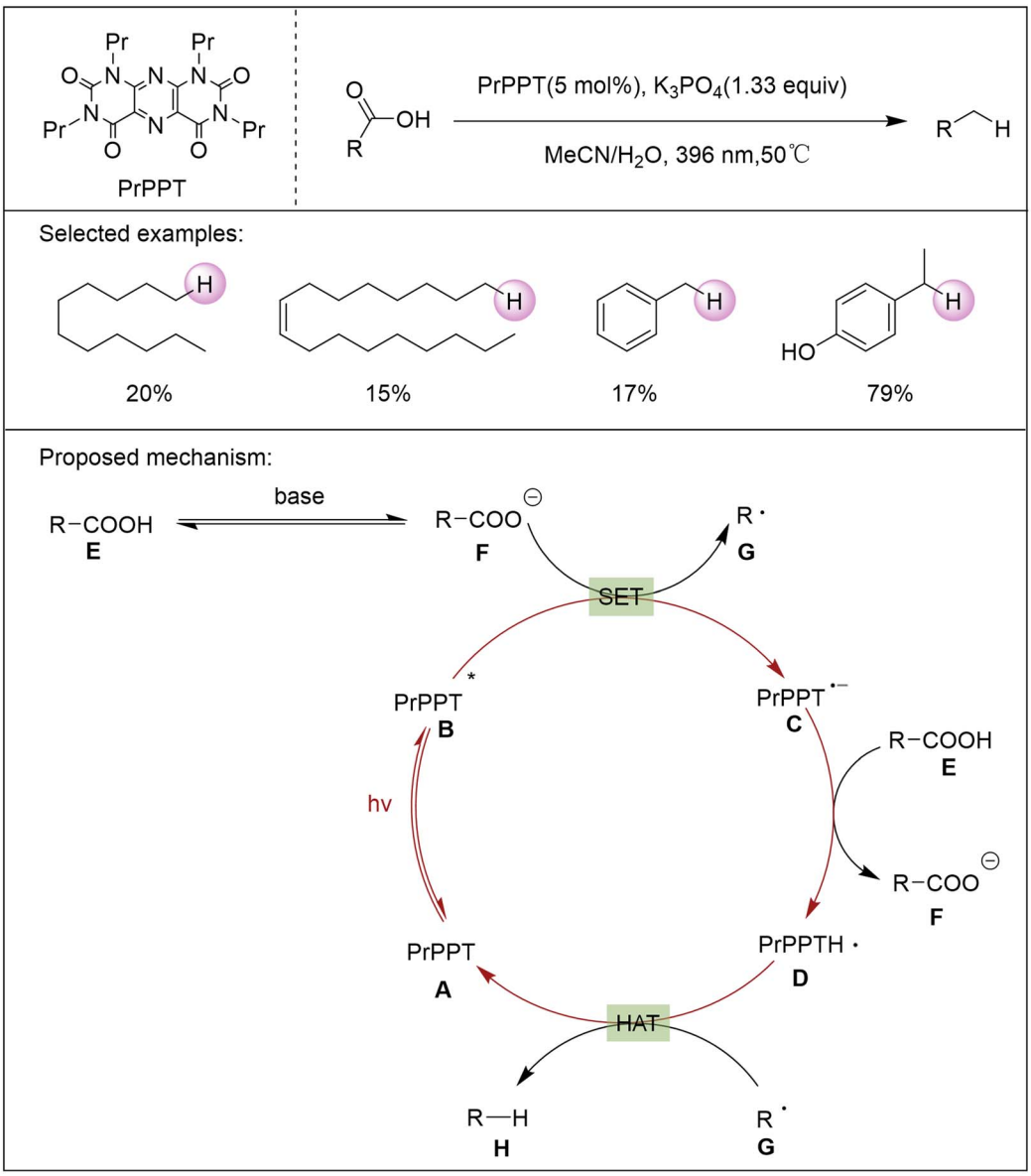

Scheme 15 Hydrodecarboxylation catalyzed by an organic pyrimidine pteridine photoredox catalyst. (This figure has been adapted/reproduced from ref. 106 with permission from Wiley, copyright 2022).

carboxylate (such as the oxidation potential of the caproate at 1.16 V). The free radical cation oxidation potential of ketones, such as diacetyl and acetophenone, is sufficient (1.28 V), but ketones with a high electron cloud density (such as electron-rich aromatic ketones) may lead to a decrease in SET oxidation efficiency due to the insufficient stability of free radical cations. Based on the experimental verification of the mechanism, the author proposes the following mechanism (Scheme 16): the ground-state ketone photocatalyst **A** becomes an excited-state **B** under visible light irradiation, and **B** exhibits strong oxidizability. The carboxylate is quickly oxidized to a free radical **F** through the SET process, and the electron is converted into a ketone free radical **C**. Then, **F** quickly removes CO_2 and converts it into an alkyl radical **G**. Finally, alkyl radical **G** and Selectfluor obtain the target product **H** through the SET pathway.

In 2025, the Deng group developed a synergistic catalyst system consisting of acridine and thiophenol. Reaction optimization significantly reduced the catalyst loading, only using 4 mol% acridine and 1 mol% thiophenol.[108] This process introduces an innovative use of waste edible oils (WCO) as the raw material. A design that obviates the requirement for subsequent processing procedures like solvent separation. Notably, when the residence time is 1 hour, the yield of C_{n-1} alkanes can exceed 90% (Scheme 17a). Nitrogen heterocyclic compounds (such as pyrazolidinone derivatives) are widely present in drug molecules with anti-inflammatory, antipyretic, analgesic and other activities. The construction of such

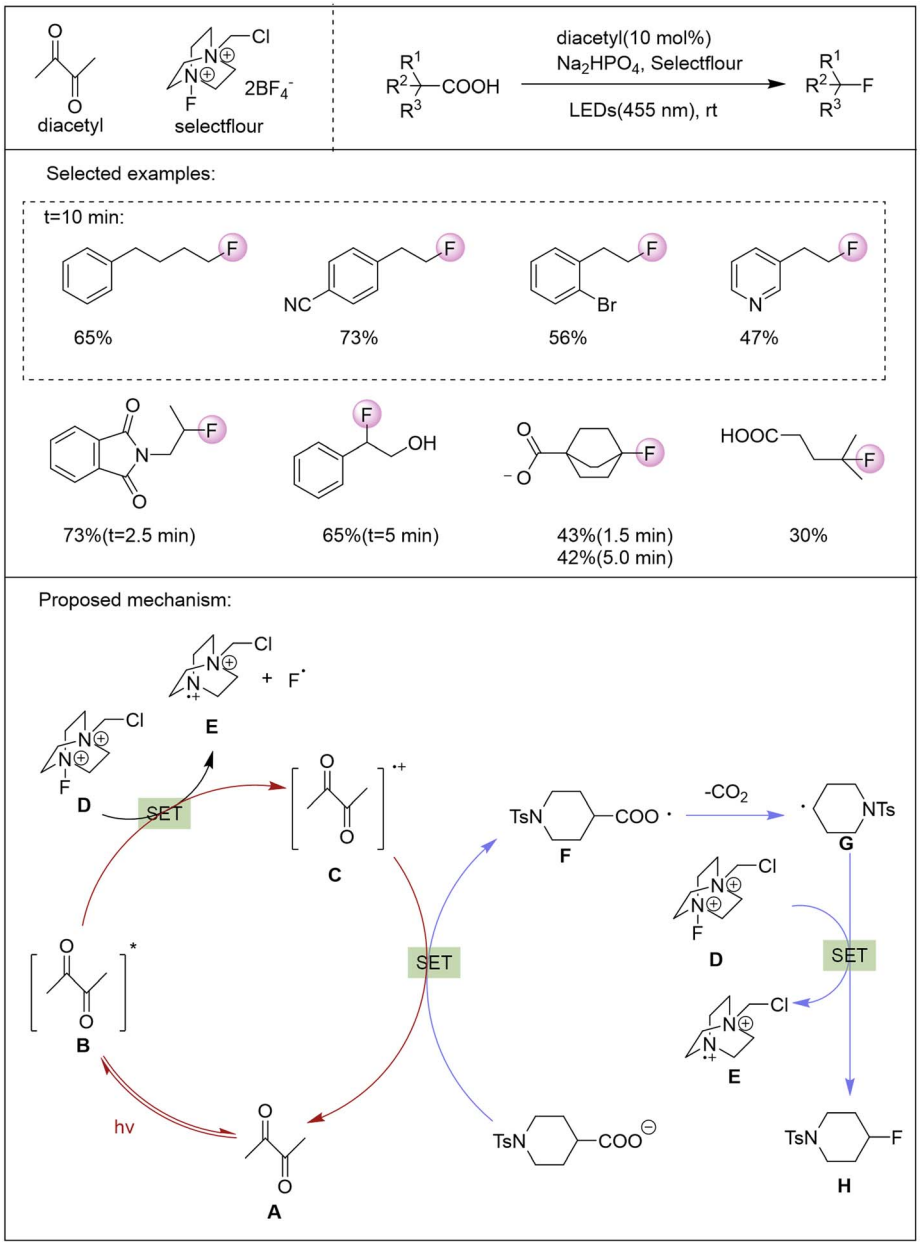

Scheme 16 Decarboxylation fluorination reaction with a ketone as a photocatalyst reported by the Zhang and colleagues. (This figure has been adapted/reproduced from ref. 107 with permission from Elsevier, copyright 2024).

skeletons by the C–H (amino) alkylation of hydrazone imines is an important strategy in modern synthesis. The Nasireddy and colleagues[109] realized the decarboxylative aminoalkylation of hydrazone imines by *N*-aryl and *N*-Boc-protected glycine derivatives for the first time using a catalytic amount of 4CzIPN. In this reaction, the 4CzIPN photocatalyst absorbs blue photons to reach the excited state to obtain a strong oxidizing ability to deoxidize carboxylate anions to form free radical cations and then removes carbon dioxide to form alkyl radicals. The alkyl radicals can be added to the hydrazone imine to form a new *N*-center free radical cation, and the electrons are finally obtained using 4CzIPN* and protonated to form the target product (Scheme 17b).

5. Semiconductor material photocatalysts

Semiconductor photocatalysis has developed rapidly, and metal oxides, sulfides and non-metallic compounds have been discovered. The material has excellent redox properties, and the controllable oxidation and reduction of the substrate can be achieved by properly adjusting the VB and CB. Aiming to address the limitations that many photocatalysts face, such as

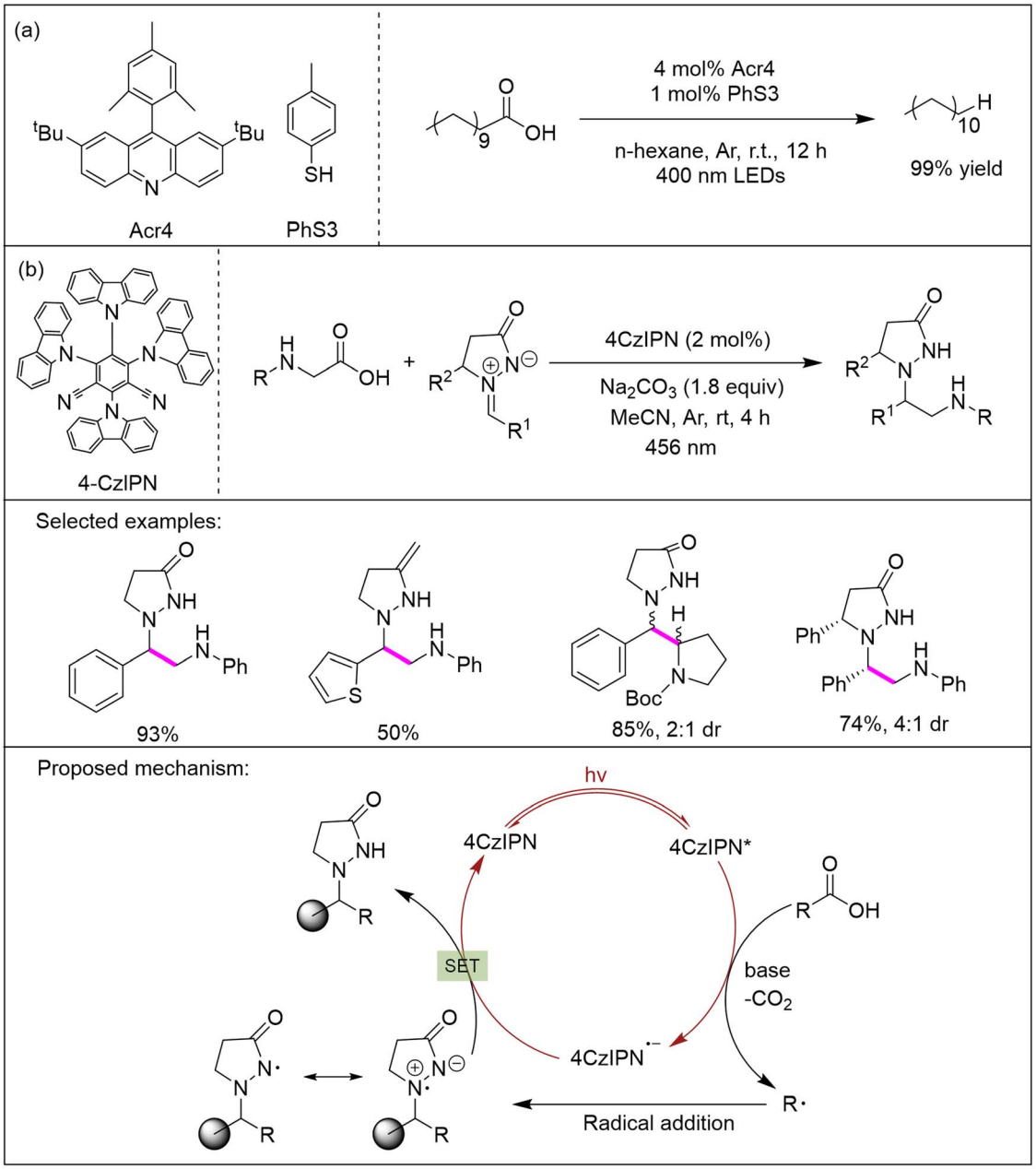

Scheme 17 (a) Hydrodecarboxylation catalyzed through a synergistic system composed of acridine and thiophenol.[108] (b) Decarboxylative aminoalkylation catalyzed by 4-CzIPN. (This figure has been adapted/reproduced from ref. 109 with permission from the American Chemical Society, copyright 2025).

a limited number of active centers, wide band gaps, low sunlight utilization rates and high recombination rates of photogenerated carriers, a variety of effective engineering modification technologies have been proposed. These include morphology and crystal structure regulation, doping induction, heterostructure fabrication with other semiconductor materials, and dye sensitization to improve photocatalytic ability and achieve the precise regulation of redox reactions. Although organic semiconductor photocatalysts have excellent light-absorption ability and structural tunability, their poor chemical stability, high exciton dissociation energy and low carrier mobility have become bottlenecks to improving performance. Future development directions include the development of efficient and stable organic–inorganic composite materials, the synergistic effect of broad spectral response and long-life carriers, and an in-depth understanding of the reaction mechanism to guide the molecular-level design of catalysts. Compared with homogeneous catalysts, heterogeneous catalysts have the advantage of easy recovery due to their insolubility.[110,111]

The boron carbonitride (BCN) photocatalyst is a metal-free heterogeneous photocatalyst with a wide adjustable band gap

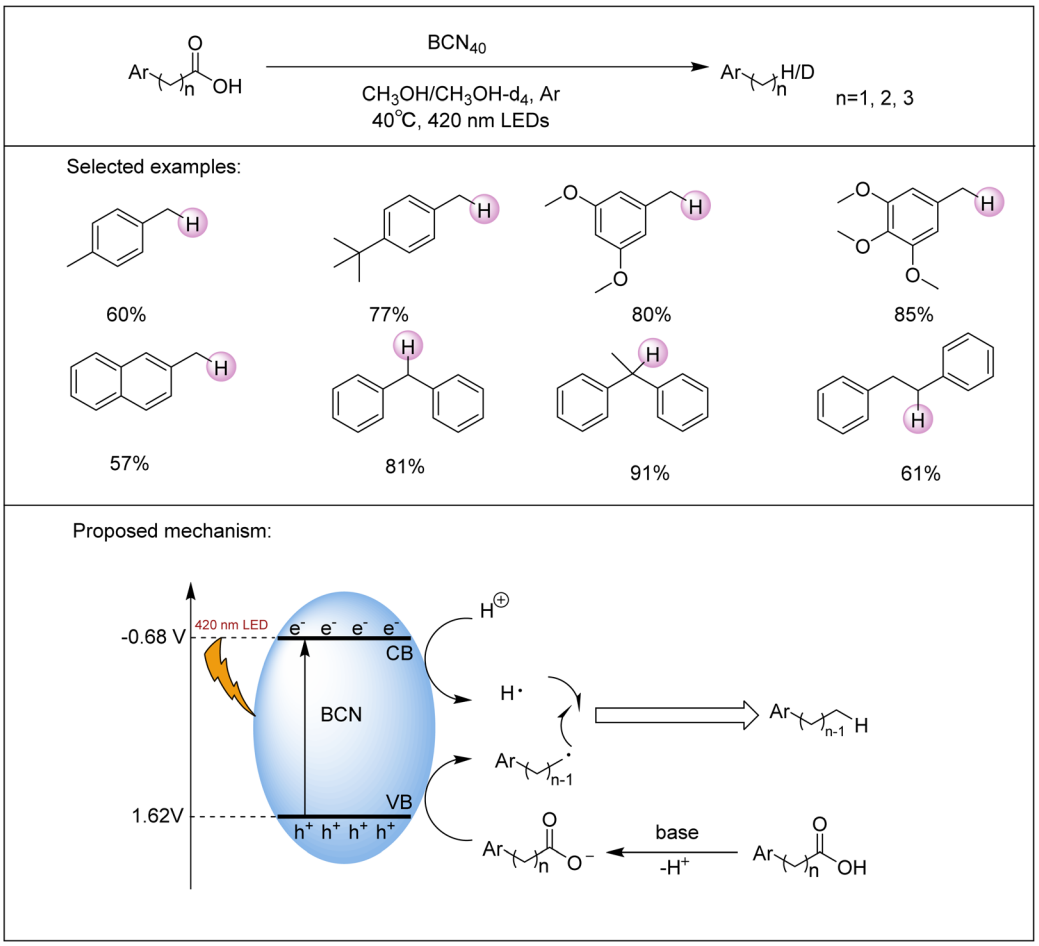

Scheme 18 BCN_{40}-mediated visible-light photocatalytic decarboxylation of carboxylic acids reported by the Shi and colleagues. (This figure has been adapted/reproduced from ref. 118 with permission from the Royal Society of Chemistry, copyright 2021).

and good visible-light response. The BCN material is composed of boron, carbon and nitrogen ternary elements, with a large specific surface area and rich active sites. The carrier separation efficiency and photocatalytic activity can be significantly improved by forming heterojunctions or doping.[112–116] In the field of photocatalytic organic synthesis, BCN photocatalysts have been able to use visible light to induce the single-electron transfer of organic halides to construct C–H, C–C and C–S bonds, and exhibit high selectivity and good cycle performance.[117] In addition, BCN is also used for sp^2 C–H bond functionalization, dehydrogenation reactions and other organic transformations. In 2021, the Shi and colleagues[118] developed a system that uses carbon-doped metal-free heterogeneous semiconductor photocatalysts (BCN) with carbon-regulated band structures and uses methanol as a hydrogen source to achieve efficient decarboxylative hydrogenation (yields reaching up to 93%) (Scheme 18). The mechanism of the reaction is as follows: BCN absorbs photons to form hole–electron pairs, and then the holes and electrons are separated and transferred to the organic substrate. First, the carboxylic acid undergoes deprotonation to form carboxylate anions; subsequently, the anions are oxidized to acyloxy radicals by photogenerated holes, and the acyloxy radicals release CO_2 to form carbon-centered radicals. In the hydrogenolysis decarboxylation reaction, the carbon-centered radical captures hydrogen atoms from methanol through a single-electron transfer pathway to obtain the final reduction product.

In 2024, the Hao group utilized the photothermal conversion effect of α-Fe_2O_3 to enable self-heating, raising the efficiency and product concentration of its photocatalytic decarboxylation to an industrial level.[119] The purpose of this reaction is to optimize the substrate adsorption mode and charge transfer path through the photothermal synergistic effect and finally realize the efficient conversion of long-chain fatty acids into C_{n-1} alkanes. Under strong visible-light excitation, α-Fe_2O_3 produces hole–electron (h^+/e^-) pairs; at low temperature, the long-chain part of the amphiphilic long-chain fatty acid is perpendicular to the interface of the polar α-Fe_2O_3 surface, which makes the photogenerated h^+/e^- difficult to approach and attack the C–COO bond, so the apparent quantum efficiency (AQE) is extremely low at room temperature. However, the high temperature generated by the incident light-induced self-heating can make the long chain of upright fatty acids spread to the surface of α-Fe_2O_3, which is convenient for the

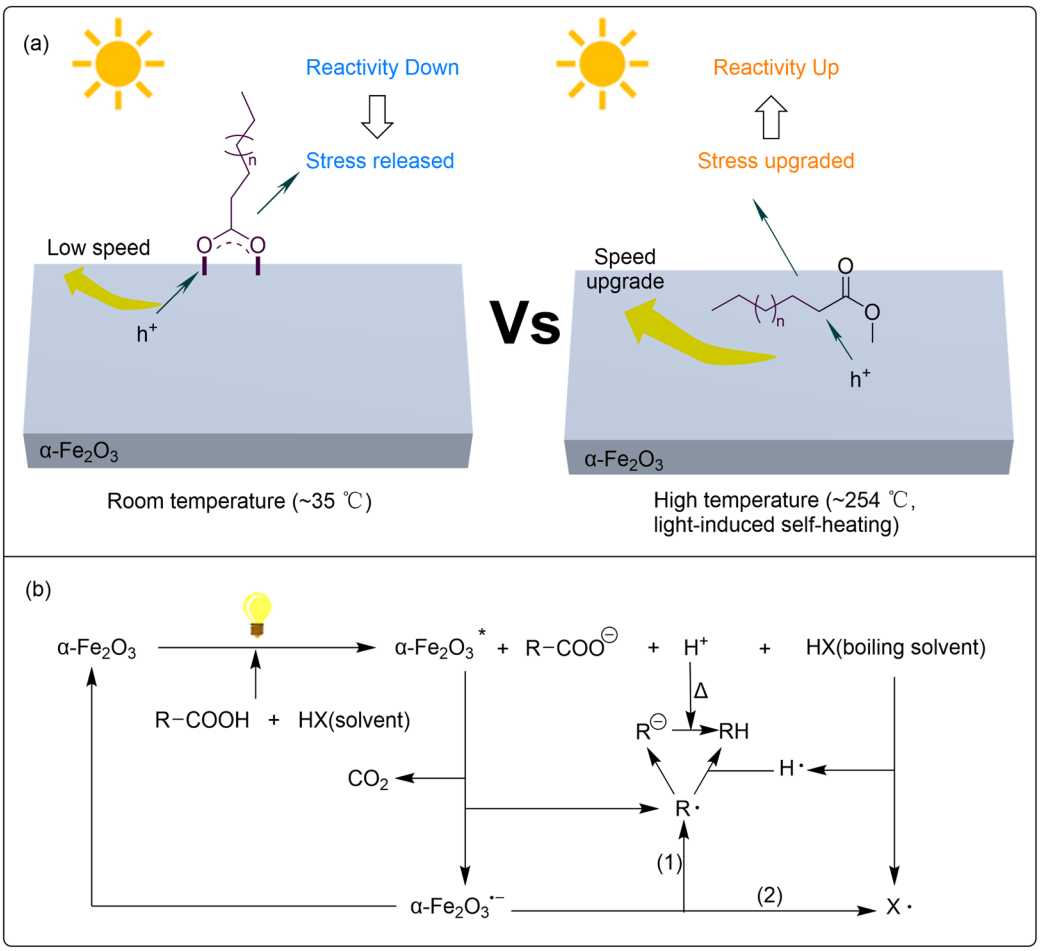

Scheme 19 Mechanism of the photocatalytic decarboxylation of fatty acids in boiling long-chain *n*-alkane solvents over α-Fe_2O_3 catalysts. (a) At high temperatures, fatty acids attach to the surface of α-Fe_2O_3, absorbing heat energy and thereby enabling hole activation; and (b) proposed overall reaction pathway: (1) major transfer direction of e^- and (2) minor transfer direction of e^-. (This figure has been adapted/reproduced from ref. 119 with permission from Elsevier, copyright 2024).

nearby h^+ to attack the C–COO bond with greater tension (Scheme 19a). In addition, with an increase in temperature, the reactivity of the photogenerated e^- changes from the PCET pathway (Scheme 19b). Obviously, the further conversion of photogenerated free electrons preferentially leads to the formation of R^-, and if the R^- intermediate is rapidly consumed, h^+/e^- recombination will be largely suppressed. Since the reaction between R^- and H^+ is directly controlled by thermodynamic collision, rather than photogenerated h^+/e^-, the reaction rate is greatly dependent on temperature. Therefore, combined with the photothermal effect of the α-Fe_2O_3 photocatalyst, the incident light energy can be effectively utilized, and the substrate conversion can be accelerated by increasing the reaction temperature. In this study, stearic acid was converted into approximately 0.5 M *n*-heptadecane in a single reaction, with a selectivity of 91%, which is far more than the concentration limit of traditional photocatalysis, which typically does not exceed the millimolar level.

In 2025, the Vilé group used carbonitride nanosheets (nCN_x)[120] prepared *via* the one-step calcination of cheap raw materials. This nCN_x, in synergy with nickel catalysis, enables the direct cross-coupling of carboxylic acids with alkyl halides. The substrate scope is broad: the method delivers high yields for common cyclic and linear α-amino acids, heteroatom-containing carboxylic acids, and drug molecules (*e.g.*, levodopa precursor, 71% yield) (Scheme 20a). The Sankar and colleagues realized the decarboxylation of readily available carboxylic acids and the oxidation of olefins and alkanes by visible light using g-C_3N_4 as a stable and recyclable catalyst.[121] This scalable method affords a range of aldehydes and ketones under mild reaction conditions, requiring only molecular oxygen as the oxidant. It is worth noting that no stoichiometric base is needed. Furthermore, the reaction proceeds efficiently even under open-air conditions and exhibits excellent activity toward diverse substrates, including phenylacetic acids, heterocyclic acetic acids, olefins, and alkanes (Scheme 20b). The Jati and colleagues developed a robust photocatalyst based on a covalent organic framework (COF),[122] which can realize the photocatalytic decarboxylative fluorination reaction of various carboxylic acids to produce alkyl fluorides with significant efficiency. The catalytic activity of an anthraquinone-based COF catalyst (TpAQ) is better than that of other β-ketoamine COFs

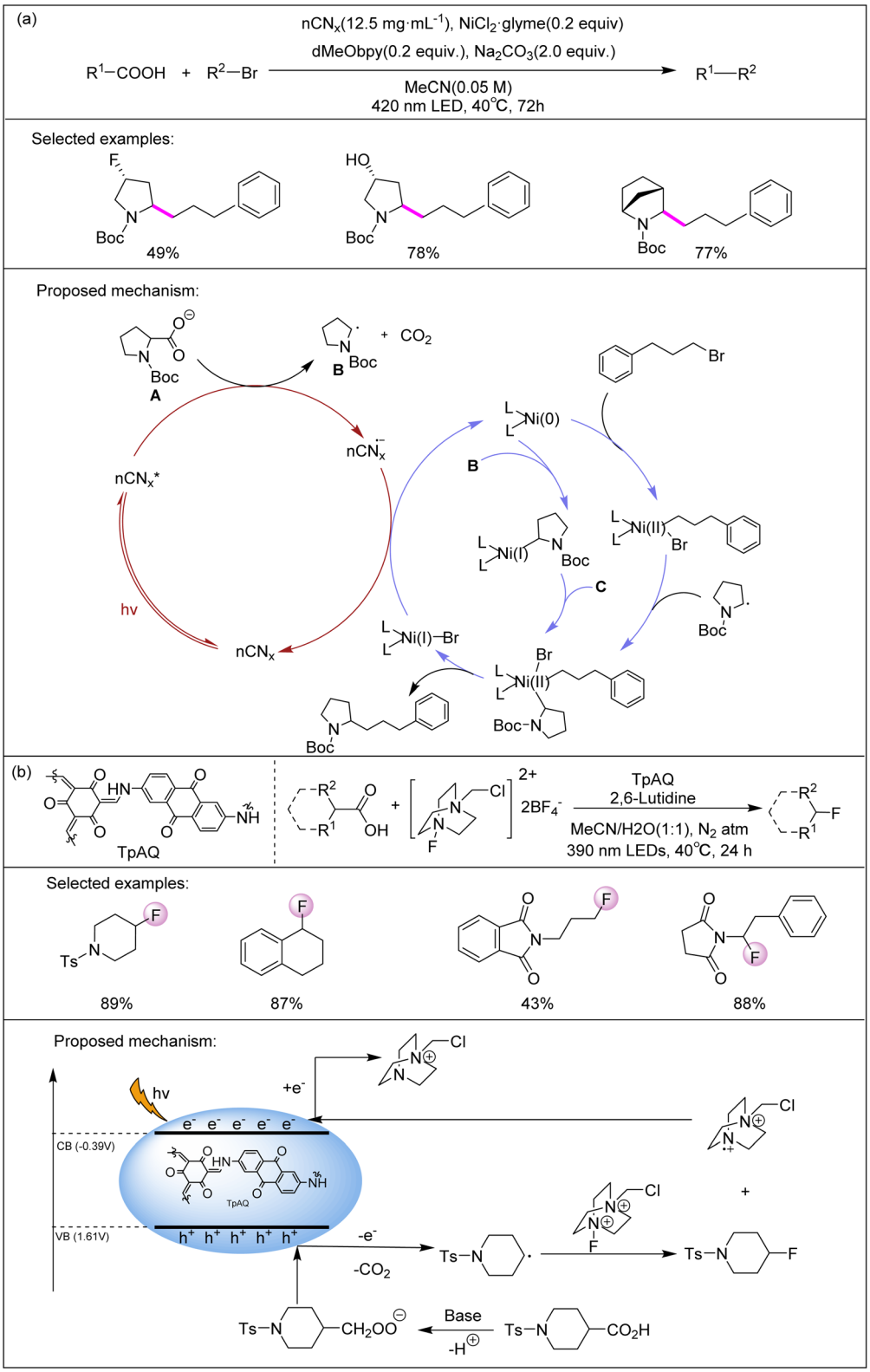

Scheme 20 (a) Cross-coupling reaction of alkyl halides and carboxylic acids catalyzed by nCN_x. (This figure has been adapted/reproduced from ref. 120 with permission from Springer Nature, copyright 2025). (b) Decarboxylation oxidation reaction using g-C_3N_4 as a photocatalyst, as reported by the Sankar and colleagues. (This figure has been adapted/reproduced from ref. 121 with permission from Wiley, copyright 2024).

with similar structures. Its β-ketoenamine skeleton, high specific surface area (1115 m^2 g^{-1}), long excited-state lifetime (3.83 ns) and efficient charge separation efficiency enable an efficient reaction. In addition, the TpAQ catalyst exhibits excellent durability, making it a sustainable and cost-effective solution. Under the irradiation of purple LED, the electrons

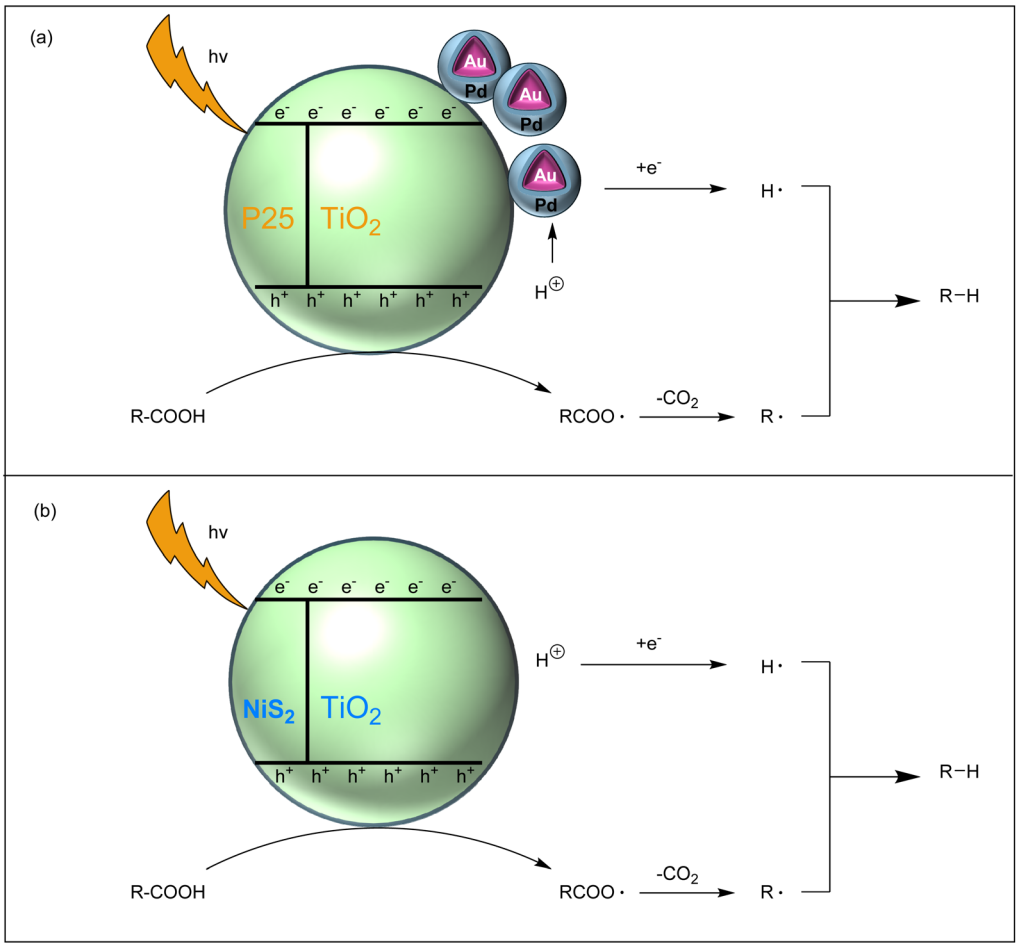

Scheme 21 (a) Proposed reaction mechanism of the composite photocatalyst 1.5Au0.8Pd/TiO_2 and (b) sulfide-modified TiO_2. (This figure has been adapted/reproduced from ref. 124 with permission from the American Chemical Society, copyright 2023).

on the VB of TpAQ are excited to the CB to form a stable hole–electron pair. At the same time, the carboxylate substrate is oxidized by the VB hole of TpAQ through the SET process in the presence of alkali. The oxidized carboxylate intermediate rapidly releases CO_2 to form alkyl radicals; the F atom is directly captured in the alkyl radical Selectfluor to form the target product alkyl fluoride, and Selectfluor is converted into a free radical cation. The conduction band electron of TpAQ needs to reduce the free radical cation generated by Selectfluor to complete the cycle, but the reaction rate of Selectfluor with the conduction band electron needs to match the fluorination rate of the alkyl radical. When the rate of free radicals generated by the substrate is too slow (such as carboxylic acids containing large sterically hindered functional groups), this leads to the accumulation of conduction band electrons and triggers the reduction of COF itself or Selectfluor decomposition. However, the valence band potential of TpAQ (1.61 V *vs.* Ag/AgCl) is only slightly higher than the oxidation potential of carboxylates (1.52 V *vs.* Ag/AgCl), and the oxidation driving force is limited. For carboxylic acids with extremely low electron cloud density (such as perfluorophenoxyacetic acid, the yield is 42%), the SET process efficiency decreases, and the yield is low. This work lays the foundation for the development of efficient and sustainable light-driven synthesis methods using COFs as photocatalysts.

TiO_2, one of the most studied photocatalysts, has shown remarkable catalytic activity in the decarboxylation of fatty acids. Through the incorporation of different supported active metals (Pt, Pd, Ru, Ni, Cu, and La), its catalytic activity can be significantly improved.[123] In 2023, Hu, García, and their colleagues compared the performance of TiO_2-supported monometallic Au or Pd catalysts with that of bimetallic Au–Pd core–shell catalysts.[124] They found that the latter exhibited significant advantages: under UV-visible light irradiation (without H_2), the conversion of hexanoic acid reached 94.7%, and the selectivity for pentane was nearly 100%, far better than that of monometallic catalysts. Such enhancement stems from the synergistic effect of Au-core/Pd-shell nanoalloys, which improves charge separation efficiency under visible-light excitation. The catalyst can efficiently convert various fatty acids and shows good stability after multiple repeated uses. Density functional theory calculations reveal that carboxylates are oxidized on TiO_2 to form alkyl radicals, which then adsorb on metal particles. The Au–Pd core–shell alloy achieves excellent catalytic performance due to its weak H adsorption and low overpotential for the hydrogen evolution reaction (Scheme 21a).

In 2024, the Guo and colleagues studied the composite photocatalyst of sulfide-modified TiO_2 (MS_2/TiO_2, M = Ni, Co, Fe).[125] Among them, NiS_2/TiO_2 achieved the efficient decarboxylation of biomass fatty acids at 10 °C under vacuum (no H_2), with a palmitic acid conversion rate of 60.2% and a pentadecane selectivity of 72.6%, significantly outperforming pure TiO_2 and other MS_2/TiO_2. The study found that the introduction of NiS_2 shifts the absorption edge to red, constructs a built-in electric field, and simultaneously enhances light absorption and the separation efficiency of photogenerated carriers, which is the major reason for the improved catalytic performance (Scheme 21b). The study emphasizes the formation of alkanes without external hydrogen sources, and it is speculated that hydrogen originates from the dissociation of fatty acids themselves.

In 2025, the Liu group developed a method for the synthesis of linear α-olefins and hydrogen by the decarboxylative olefination of fatty acids in an acetonitrile solvent through the synergistic effect of Ag/TiO_2 and a Co^{3+} cocatalyst.[126] Comprehensive characterization and density functional theory (DFT) calculations show that the loading of Ag nanoparticles enhances the decarboxylation activity of TiO_2. Due to the weak adsorption characteristics of Ag nanoparticles on alkyl radicals and the solvent stabilization effect, the alkyl radical intermediates can be quickly desorbed and diffused from the Ag/TiO_2 catalytic interface and captured by the molecular Co^{3+} cocatalyst, thereby generating linear α-olefins and hydrogen (Scheme 22a). In 2026, the Wang group achieved the efficient conversion of fatty acid derivatives *via* photocatalytic decarboxylative hydrogenation or C–C coupling using Rh co-catalyst-modified TiO_2.[127] The oxidized Rh(RhO) acts as a hole cocatalyst to promote the combination of H˙ and R˙ and drive the decarboxylation hydrogenation reaction. On the contrary, metal Rh acts as an electron cocatalyst to enhance the self-binding of H˙ to generate H_2, while allowing the remaining R˙ to undergo C–C coupling. By adjusting the valence state of Rh, the spatial separation of free radical intermediates is achieved, thereby guiding the reaction path (Scheme 22b).

In 2026, the Sun group adopted the photo-induced ligand exchange (PILE) strategy, using the lone pair electrons of the carbon nitride-rich N atom to anchor the Fe atom and promoting ligand exchange under light to form atomically dispersed Fe–N_2 sites.[128] The catalyst has two electron transfer mechanisms of homogeneous and heterogeneous catalyses and is capable of LMCT (activated carboxylic acid) and SET (activated electron-deficient olefin) without additional ligands or sacrificial reagents. Here, the carboxylic acid molecule first coordinates with the Fe(III) site on the catalyst. Under illumination, the electrons directly transition from the orbital of the carboxylic acid ligand to the orbital of the Fe metal center, resulting in the homolysis of the Fe–O bond, generation of alkyl radicals and release of CO_2. This step bypasses the limitation that the semiconductor band is unable to directly oxidize the alkyl carboxylic acid with high oxidation potential (Scheme 23). Ibuprofen derivatives can be obtained in 99% yield using only a catalyst and solvent, showing the potential for drug modification.

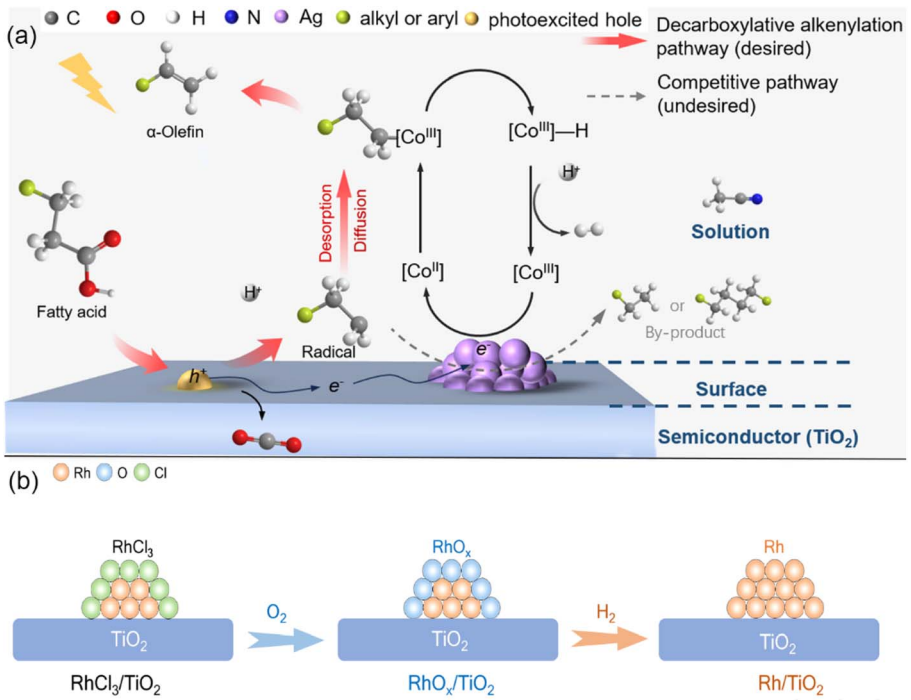

Scheme 22 (a) Proposed mechanism for the synthesis of LAOs from fatty acids catalyzed by Ag/TiO_2 and molecular Co^{III} cocatalysts. (This figure has been adapted/reproduced from ref. 126 with permission from the American Chemical Society, copyright 2025). (b) Scheme of the preparation of the RhO_x/TiO_2 and Rh/TiO_2 samples. (This figure has been adapted/reproduced from ref. 127 with permission from the American Chemical Society, copyright 2026).

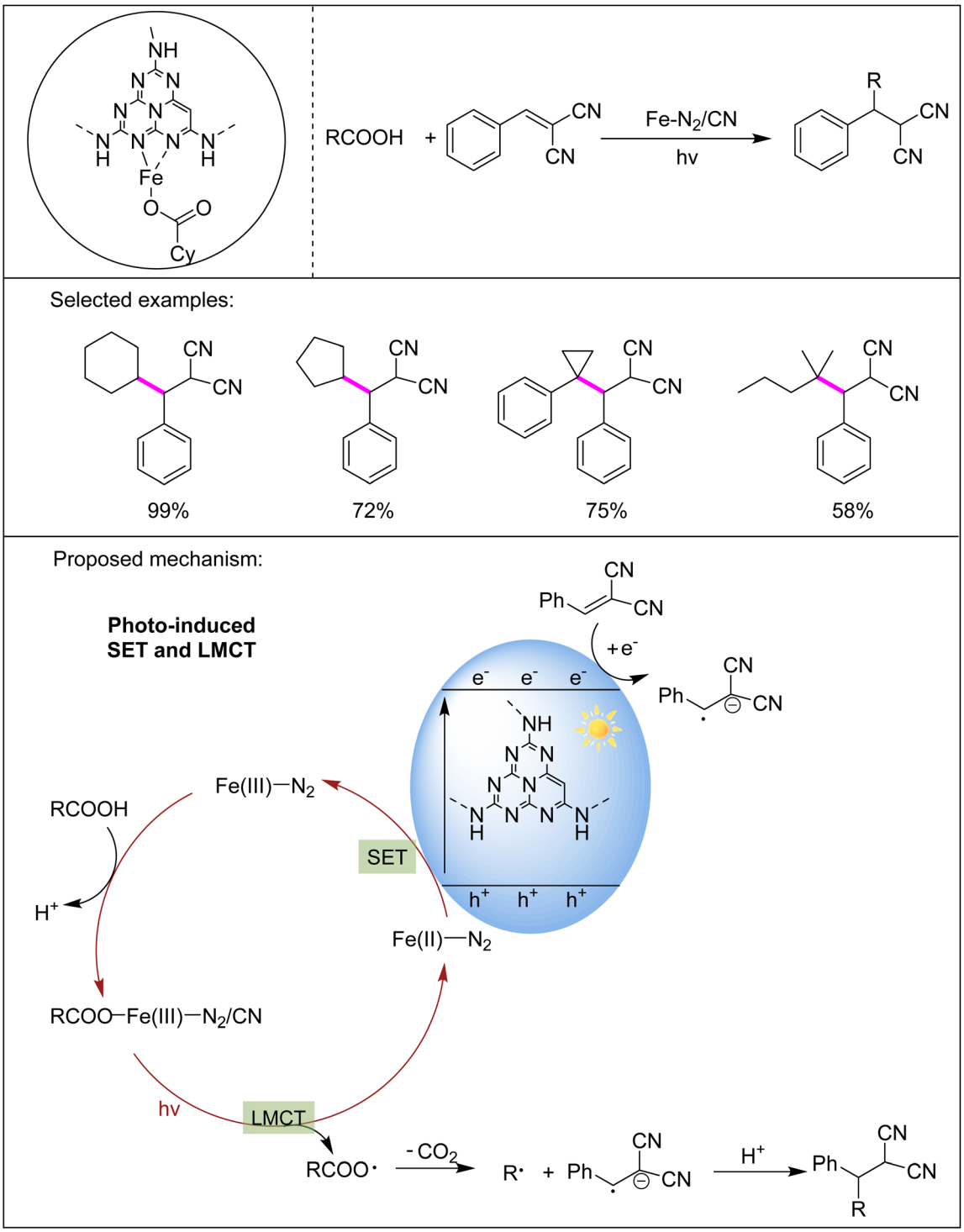

Scheme 23 Decarboxylative coupling reaction catalyzed by Fe–N_2/CN.[128]

6. Conclusions and outlook

The radical decarboxylative functionalization of carboxylic acids is a powerful and versatile strategy in organic synthesis, enabling the conversion of abundant natural carboxylic acid resources into high-value chemicals. In summary, various photocatalysts have been developed to generate alkyl radicals *via* decarboxylation, followed by diverse functionalization processes, such as protonation, elimination and coupling. However, this field still faces several challenges, including the decarboxylation of carboxylic acids bearing specific functional groups, chemoselectivity and reactivity of alkyl radicals, efficient control of stereoselectivity in radical alkylation reactions, and development of visible-light catalytic systems. In addition,

the performance of the currently reported photocatalysts for C(sp^3)-carboxylic acid decarboxylation is mainly reflected in the yield and selectivity. Quantum efficiency is also an important parameter for evaluating photocatalysts. Therefore, improving the quantum efficiency of photocatalysts is vital. In addition, there are a variety of photocatalysts that can respond to stronger penetration depths and milder near-infrared light (NIR) reaction conditions, including MOFs, organic molecular photosensitizers, and nanocrystalline composites. These materials achieve effective photocatalytic activity by directly absorbing NIR light or using a two-photon excitation mechanism. Although the decarboxylation reaction driven by low-energy NIR and infrared light still faces the challenge of excitation efficiency and mechanism understanding, it is believed that the design of new materials and multiple excitation strategies will provide strong support for the realization of efficient and highly selective near-infrared photocatalytic decarboxylation in the future.

Conflicts of interest

The authors declare no conflicts of interest.

Data availability

No primary research results, software or code have been included and no new data were generated or analysed as part of this review.

Acknowledgements

This work was financially supported by the Science and Technology Plan Key Project of Hunan Province (2020GK2100) and the SRF of the Hunan Provincial Education Department (25A0036).

References

1 N. Dahmen, I. Lewandowski, S. Zibek, *et al.*, Integrated lignocellulosic value chains in a growing bioeconomy: Status quo and perspectives, *GCB Bioenergy*, 2019, **11**(1), 107–117, DOI: 10.1111/gcbb.12586.

2 V. Ashokkumar, R. Venkatkarthick, S. Jayashree, *et al.*, Recent advances in lignocellulosic biomass for biofuels and value-added bioproducts-a critical review, *Bioresour. Technol.*, 2022, **344**, 126195, DOI: 10.1016/j.biortech.2021.126195.

3 N. Taufiqurrahmi and S. Bhatia, Catalytic cracking of edible and non-edible oils for the production of biofuels, *Energy Environ. Sci.*, 2011, **4**(4), 1087, DOI: 10.1039/c0ee00460j.

4 U. Biermann, U. T. Bornscheuer, I. Feussner, *et al.*, Fatty acids and their derivatives as renewable platform molecules for the chemical industry, *Angew. Chem., Int. Ed.*, 2021, **60**(37), 20144–20165, DOI: 10.1002/anie.202100778.

5 Z. Elahi, F. Mohd Jakarni, R. Muniandy, *et al.*, Waste cooking oil as a sustainable bio modifier for asphalt modification: a review, *Sustainability*, 2021, **13**(20), 11506, DOI: 10.3390/su132011506.

6 S. Foteinis, E. Chatzisymeon, A. Litinas, *et al.*, Used-cooking-oil biodiesel: life cycle assessment and comparison with first- and third-generation biofuel, *Renewable Energy*, 2020, **153**, 588–600, DOI: 10.1016/j.renene.2020.02.022.

7 J. Li, L. Lin, T. Ju, *et al.*, Microwave-assisted pyrolysis of solid waste for production of high-value liquid oil, syngas, and carbon solids: A review, *Renew. Sustain. Energy Rev.*, 2024, **189**, 113979, DOI: 10.1016/j.rser.2023.113979.

8 S. Van Dyk, J. Su, J. D. Mcmillan, *et al.*, Potential synergies of drop-in biofuel production with further co-processing at oil refineries, *Biofuel Bioprod. Biorefining*, 2019, **13**(3), 760–775, DOI: 10.1002/bbb.1974.

9 J. W. Na, J.-C. Lee and H.-W. Kim, Biodiesel production from waste cooking grease: optimization and comparative productivity assessment, *KSCE J. Civ. Eng.*, 2019, **23**(3), 1000–1006, DOI: 10.1007/s12205-019-0827-2.

10 Z. Huang, Z. Zhao, C. Zhang, *et al.*, Enhanced photocatalytic alkane production from fatty acid decarboxylation via inhibition of radical oligomerization, *Nat. Catal.*, 2020, **3**(2), 170–178, DOI: 10.1038/s41929-020-0423-3.

11 X. Li, Y. Peng, Z. Huang, *et al.*, Combined hydrogen and alkane production by photocatalytic decarboxylative c–c homocoupling of fatty acid by constructing a hydrogen-deficient catalytic interface, *ACS Catal.*, 2024, **14**(5), 3675–3686, DOI: 10.1021/acscatal.3c06070.

12 F. Li, Y. Sui, K. Lin, *et al.*, Photo-driven decarboxylation for sustainable biofuel production: a review on harnessing the potential of fatty acid decarboxylases, *Chem. Commun.*, 2025, **61**(93), 18273–18288, DOI: 10.1039/D5CC02448J.

13 S. B. Beil, T. Q. Chen, N. E. Intermaggio, *et al.*, Carboxylic acids as adaptive functional groups in metallaphotoredox catalysis, *Acc. Chem. Res.*, 2022, **55**(23), 3481–3494, DOI: 10.1021/acs.accounts.2c00607.

14 M. Roucan, M. Kielmann, S. J. Connon, *et al.*, Conformational control of nonplanar free base porphyrins: towards bifunctional catalysts of tunable basicity, *Chem. Commun.*, 2018, **54**(1), 26–29, DOI: 10.1039/C7CC08099A.

15 G. Laudadio, M. D. Palkowitz, T. El-Hayek Ewing, *et al.*, Decarboxylative cross-coupling: a radical tool in medicinal chemistry, *ACS Med. Chem. Lett.*, 2022, **13**(9), 1413–1420, DOI: 10.1021/acsmedchemlett.2c00286.

16 J. D. Tibbetts, H. E. Askey, Q. Cao, *et al.*, Decarboxylative, radical C–C bond formation with alkyl or aryl carboxylic acids: recent advances, *Synthesis*, 2023, **55**(20), 3239–3250, DOI: 10.1055/a-2081-1830.

17 J. Wang, S. Bai, C. Yang, *et al.*, Enantioselective decarboxylative C(sp^3)-C(sp^3) cross-coupling of aliphatic redox-active esters with *gem*-borazirconocene alkanes, *J. Am. Chem. Soc.*, 2024, **146**(39), 27070–27079, DOI: 10.1021/jacs.4c09245.

18 S. K. Parida, T. Mandal, S. Das, *et al.*, Single electron transfer-induced redox processes involving *N* -(Acyloxy)

phthalimides, *ACS Catal.*, 2021, **11**(3), 1640–1683, DOI: 10.1021/acscatal.0c04756.
19 M. Wang, H. Zhou and F. Wang, Photocatalytic production of syngas from biomass, *Acc. Chem. Res.*, 2023, **56**(9), 1057–1069, DOI: 10.1021/acs.accounts.3c00039.
20 D. Saha, Catalytic enantioselective radical transformations enabled by visible light, *Chem.–Asian J.*, 2020, **15**(14), 2129–2152, DOI: 10.1002/asia.202000525.
21 A. M. De Azevedo, J. G. L. De Araujo, M. D. S. B. Da Silva, *et al.*, Photocatalyzed hydrodecarboxylation of fatty acids: a prospective method to produce drop-in biofuels, *RSC Adv.*, 2024, **14**(15), 10755–10760, DOI: 10.1039/D4RA01166J.
22 C.-Q. Deng and J. Deng, Advances of the past 12 years in decarboxylation of biomass carboxylic acids to biofuels and high-value chemicals via photo- or electrocatalysis, *Green Chem.*, 2025, **27**(2), 275–292, DOI: 10.1039/D4GC04788E.
23 J. Tu, Z. Shen and B. Huang, Light-induced direct decarboxylative functionalization of aromatic carboxylic acids, *Adv. Synth. Catal.*, 2024, **366**(21), 4263–4273, DOI: 10.1002/adsc.202400573.
24 S. Mondal, S. Mandal, S. Mondal, *et al.*, Photocatalytic decarboxylation of free carboxylic acids and their functionalization, *Chem. Commun.*, 2024, **60**(72), 9645–9658, DOI: 10.1039/D4CC03189J.
25 A. Jati, A. K. Mahato, D. Chanda, *et al.*, Photocatalytic decarboxylative fluorination by quinone-based isoreticular covalent organic frameworks, *J. Am. Chem. Soc.*, 2024, **146**(34), 23923–23932, DOI: 10.1021/jacs.4c06510.
26 Y. Xu, H. Yang, J. Wang, *et al.*, Synergistic cobalt and cerium LMCT photocatalysis for decarboxylative heck type reaction facilitated by efficient acceptorless dehydrogenation, *Chin. J. Chem.*, 2025, **43**(24), 3453–3460, DOI: 10.1002/cjoc.70259.
27 N. Xiong, Y. Li and R. Zeng, Merging photoinduced iron-catalyzed decarboxylation with copper catalysis for C–N and C–C couplings, *ACS Catal.*, 2023, **13**(3), 1678–1685, DOI: 10.1021/acscatal.2c05293.
28 L. McMurray, T. M. McGuire and R. L. Howells, Recent advances in photocatalytic decarboxylative coupling reactions in medicinal chemistry, *Synthesis*, 2020, **52**(12), 1719–1737, DOI: 10.1055/s-0039-1690843.
29 S. Tamaki, T. Kusamoto and H. Tsurugi, Decarboxylative functionalization of carboxylic acids with easily oxidizable, unstable, and difficult substituents under visible light irradiation, *ChemCatChem*, 2025, **17**(8), e202402106, DOI: 10.1002/cctc.202402106.
30 X. Liu, Z. Chen, S. Lu, *et al.*, Heterogeneous photocatalytic conversion of biomass to biofuels: a review, *Chem. Eng. J.*, 2023, **476**, 146794, DOI: 10.1016/j.cej.2023.146794.
31 G. Zhang, Y. Pei, J. Wang, *et al.*, Copper-catalyzed asymmetric cyanation of propargylic radicals via direct decarboxylation of propargylic carboxylic acids, *Org. Lett.*, 2023, **25**(27), 5006–5010, DOI: 10.1021/acs.orglett.3c01637.
32 D. Yang, Y.-T. Mei, Z.-Y. Guo, *et al.*, Decarboxylative alkylation of morita–baylis–hillman acetates with aliphatic acids via photochemical iron-mediated ligand-to-metal charge transfer, *J. Org. Chem.*, 2025, **90**(10), 3665–3672, DOI: 10.1021/acs.joc.4c03047.
33 J. Wang, Z. Wang, K. Dai, *et al.*, Review on inorganic–organic S-scheme photocatalysts, *J. Mater. Sci. Technol.*, 2023, **165**, 187–218, DOI: 10.1016/j.jmst.2023.03.067.
34 C. Song, H.-H. Zhang and S. Yu, Regio- and enantioselective decarboxylative allylic benzylation enabled by dual palladium/photoredox catalysis, *ACS Catal.*, 2022, **12**(2), 1428–1432, DOI: 10.1021/acscatal.1c05461.
35 Y. Sakakibara, E. Ito, T. Fukushima, *et al.*, Late-Stage functionalization of arylacetic acids by photoredox-catalyzed decarboxylative carbon–heteroatom bond formation, *Chem.—Eur. J.*, 2018, **24**(37), 9254–9258, DOI: 10.1002/chem.201802143.
36 J. Zhang and C. Zhao, Development of a bimetallic Pd-Ni/HZSM-5 catalyst for the tandem limonene dehydrogenation and fatty acid deoxygenation to alkanes and arenes for use as biojet fuel, *ACS Catal.*, 2016, **6**(7), 4512–4525, DOI: 10.1021/acscatal.6b00520.
37 S. Lestari, P. Mäki-Arvela, J. Beltramini, *et al.*, Transforming triglycerides and fatty acids into biofuels, *ChemSusChem*, 2009, **2**(12), 1109–1119, DOI: 10.1002/cssc.200900107.
38 S. Yang, Y. Morita, Y. Nakamura, *et al.*, Tuning photoredox catalysis of ruthenium with palladium: synthesis of heterobimetallic Ru–Pd complexes that enable efficient photochemical reduction of CO_2, *J. Am. Chem. Soc.*, 2024, **146**(18), 12288–12293, DOI: 10.1021/jacs.3c14338.
39 T. Huang, P. Du and Y. Lin, Recent advances in photoactive first-row transition metal complexes for organic synthesis, *Chin. J. Chem.*, 2025, **43**(19), 2566–2587, DOI: 10.1002/cjoc.70135.
40 R. Tang, Q. Wan, T.-L. Lam, *et al.*, Copper(I)-based metal-metal-to-ligand charge transfer excited state with halogen-atom transfer photo-reactivity and photocatalysis, *Chem*, 2024, **10**(9), 2807–2828, DOI: 10.1016/j.chempr.2024.05.003.
41 Z. Nie, C. Sui, X. Xie, *et al.*, Fe vacancies in FeOCl enhanced reactive oxygen species generation for photocatalytic elimination of emerging pollutants, *Appl. Catal. B Environ. Energy*, 2024, **347**, 123819, DOI: 10.1016/j.apcatb.2024.123819.
42 D.-S. Zhang, L. Wang, X. Zhang, *et al.*, Emerging inorganic–organic hybrid photocatalysts for solar-driven overall water splitting: progress and perspectives, *Chem. Soc. Rev.*, 2025, **54**, 9978–10005, DOI: 10.1039/D5CS00378D.
43 M. Wu, J. Sun, Y. Cui, *et al.*, Active learning-driven discovery of donor-acceptor covalent triazine frameworks for high-performance photocatalysts, *Adv. Funct. Mater.*, 2025, 2505234, DOI: 10.1002/adfm.202505234.
44 L. Deng and J. Qu, Design of novel phenothiazine-based push-pull photoinitiators for visible light with high activity, good solubility and low migration, *Prog. Org. Coat.*, 2023, **183**, 107766, DOI: 10.1016/j.porgcoat.2023.107766.
45 X. Yuan, H.-B. Fan, J. Liu, *et al.*, Recent advances in photoredox catalytic transformations by using

continuous-flow technology, *Chin. J. Catal.*, 2023, **50**, 175–194, DOI: 10.1016/S1872-2067(23)64447-X.

46 F. Nekouei, T. Wang, F. Keshtpour, *et al.*, Effective redox reaction in a three-body smart photocatalyst through multi-interface modulation of organic semiconductor junctioned with metal and inorganic semiconductor, *Appl. Catal. B Environ. Energy*, 2024, **351**, 123974, DOI: 10.1016/j.apcatb.2024.123974.

47 S. Wang, J. Wang, Y. Wang, *et al.*, Insight into the selectivity-determining step of various photocatalytic CO_2 reduction products by inorganic semiconductors, *ACS Catal.*, 2024, **14**(14), 10760–10788, DOI: 10.1021/acscatal.4c01712.

48 Y. Xu, C. Shen and K. Dong, Enantioselective decarboxylative hydrogen-atom transfer reaction, *J. Am. Chem. Soc.*, 2025, **147**(7), 6259–6267, DOI: 10.1021/jacs.4c18464.

49 C. Ji, Y. Lu, S. Xia, *et al.*, Photoinduced late-stage radical decarboxylative and deoxygenative coupling of complex carboxylic acids and their derivatives, *Angew. Chem., Int. Ed.*, 2025, **64**(9), e202423113, DOI: 10.1002/anie.202423113.

50 X.-K. Qi, L.-J. Yao, M.-J. Zheng, *et al.*, Photoinduced hydrodifluoromethylation and hydromethylation of alkenes enabled by ligand-to-iron charge transfer mediated decarboxylation, *ACS Catal.*, 2024, **14**(3), 1300–1310, DOI: 10.1021/acscatal.3c05541.

51 Z.-L. Xie, N. Gupta, J. Niklas, *et al.*, Photochemical charge accumulation in a heteroleptic copper(I)-anthraquinone molecular dyad via proton-coupled electron transfer, *Chem. Sci.*, 2023, **14**(37), 10219–10235, DOI: 10.1039/D3SC03428C.

52 J. Kosco, F. Moruzzi, B. Willner, *et al.*, Photocatalysts based on organic semiconductors with tunable energy levels for solar fuel applications, *Adv. Energy Mater.*, 2020, **10**(39), 2001935, DOI: 10.1002/aenm.202001935.

53 O. Sadek, M. Abdellaoui, A. Millanvois, *et al.*, Organometallic catalysis under visible light activation: benefits and preliminary rationales, *Photochem. Photobiol. Sci.*, 2022, **21**(4), 585–606, DOI: 10.1007/s43630-022-00181-8.

54 K. P. S. Cheung, S. Sarkar and V. Gevorgyan, Visible light-induced transition metal catalysis, *Chem. Rev.*, 2022, **122**(2), 1543–1625, DOI: 10.1021/acs.chemrev.1c00403.

55 K. P. S. Cheung and V. Gevorgyan, Illuminating palladium catalysis, *Acc. Chem. Res.*, 2025, **58**(6), 861–876, DOI: 10.1021/acs.accounts.4c00815.

56 C. S. Kuehner, A. G. Hill, C. F. Harris, *et al.*, Catalytic C–H trifluoromethylation of arenes and heteroarenes via visible light photoexcitation of a Co(III)–CF_3 complex, *ACS Catal.*, 2023, **13**(20), 13607–13617, DOI: 10.1021/acscatal.3c03832.

57 L. Ibáñez-Ibáñez, A. Lázaro, C. Mejuto, *et al.*, Visible light harvesting alkyne hydrosilylation mediated by pincer platinum complexes, *J. Catal.*, 2023, **428**, 115155, DOI: 10.1016/j.jcat.2023.115155.

58 X. Sun, J. Chen and T. Ritter, Catalytic dehydrogenative decarboxyolefination of carboxylic acids, *Nat. Chem.*, 2018, **10**(12), 1229–1233, DOI: 10.1038/s41557-018-0142-4.

59 V. T. Nguyen, V. D. Nguyen, G. C. Haug, *et al.*, Alkene synthesis by photocatalytic chemoenzymatically compatible dehydrodecarboxylation of carboxylic acids and biomass, *ACS Catal.*, 2019, **9**(10), 9485–9498, DOI: 10.1021/acscatal.9b02951.

60 N. A. Till, R. T. Smith and D. W. C. MacMillan, Decarboxylative hydroalkylation of alkynes, *J. Am. Chem. Soc.*, 2018, **140**(17), 5701–5705, DOI: 10.1021/jacs.8b02834.

61 A. Noble, R. S. Mega, D. Pflästerer, *et al.*, Visible-light-mediated decarboxylative radical additions to vinyl boronic esters: rapid access to γ-amino boronic esters, *Angew. Chem., Int. Ed.*, 2018, **57**(8), 2155–2159, DOI: 10.1002/anie.201712186.

62 H. Yue, C. Zhu, R. Kancherla, *et al.*, Regioselective hydroalkylation and arylalkylation of alkynes by photoredox/Nickel dual catalysis: application and mechanism, *Angew. Chem., Int. Ed.*, 2020, **59**(14), 5738–5746, DOI: 10.1002/anie.201914061.

63 G. Ernouf, E. Chirkin, L. Rhyman, *et al.*, Photochemical strain-release-driven cyclobutylation of C(sp^3)-centered radicals, *Angew. Chem., Int. Ed.*, 2020, **59**(7), 2618–2622, DOI: 10.1002/anie.201908951.

64 R. D. Taylor, M. MacCoss and A. D. G. Lawson, Rings in drugs: miniperspective, *J. Med. Chem.*, 2014, **57**(14), 5845–5859, DOI: 10.1021/jm4017625.

65 S. N. Khan, M. K. Zaman, R. Li, *et al.*, A general method for photocatalytic decarboxylative hydroxylation of carboxylic acids, *J. Org. Chem.*, 2020, **85**(7), 5019–5026, DOI: 10.1021/acs.joc.0c00312.

66 P. Li, J. R. Zbieg and J. A. Terrett, A platform for decarboxylative couplings via photoredox catalysis: direct access to carbocations from carboxylic acids for carbon–oxygen bond formation, *ACS Catal.*, 2021, **11**(17), 10997–11004, DOI: 10.1021/acscatal.1c03251.

67 R. Song, Z. Lian, W. Feng, *et al.*, Palladium-catalyzed decarboxylative *O*-allylation of phenols with γ-methylidene-δ-valerolactones, *Org. Chem. Front.*, 2022, **9**(16), 4365–4371, DOI: 10.1039/D2QO00444E.

68 W. Feng, X. Wu, R. Song, *et al.*, Phenol-mediated decarboxylative proton transfer of γ-methylidene-δ-valerolactones: an approach towards (*E*)-2,4-pentadienoates, *Org. Chem. Front.*, 2024, **11**(7), 2015–2020, DOI: 10.1039/D3QO01766D.

69 R. Song, J. Li, L. Li, *et al.*, Palladium/photoredox catalysis for a decarboxylative radical C(sp^3)–C(sp^3) cross-coupling reaction of γ-methylidene-δ-valerolactones with alkyl carboxylic acids, *Org. Chem. Front.*, 2025, **10**, 1039, DOI: 10.1039/D5QO01005E.

70 N. Wei and S. B. Beil, Nickel-photocatalytic decarboxylative oxidation, *ChemPhotoChem*, 2025, e202500241, DOI: 10.1002/cptc.202500241.

71 J. Wu, C. Shu, Z. Li, *et al.*, Photoredox-catalyzed decarboxylative bromination, chlorination and thiocyanation using inorganic salts, *Angew. Chem., Int. Ed.*, 2023, **62**(38), e202309684, DOI: 10.1002/anie.202309684.

72 S.-C. Kao, K.-J. Bian, X.-W. Chen, *et al.*, Photochemical iron-catalyzed decarboxylative azidation via the merger of ligand-to-metal charge transfer and radical ligand transfer catalysis, *[J]. Chem Catalysis*, 2023, **3**(6), 100603, DOI: 10.1016/j.checat.2023.100603.

73 Y. Zhang, J. Qian, M. Wang, *et al.*, Visible-light-induced decarboxylative fluorination of aliphatic carboxylic acids catalyzed by iron, *Org. Lett.*, 2022, **24**(32), 5972–5976, DOI: 10.1021/acs.orglett.2c02242.

74 R. Kancherla, K. Muralirajan, A. Sagadevan, *et al.*, Visible light-induced excited-state transition-metal catalysis, *Trends Chem.*, 2019, **1**(5), 510–523, DOI: 10.1016/j.trechm.2019.03.012.

75 C. T. Ludwig, I. A. Owolabi, L. W. Evans, *et al.*, Wavelength-selective reactivity of Iron(III) halide salts in photocatalytic C–H functionalization, *J. Org. Chem.*, 2025, **90**(9), 3404–3411, DOI: 10.1021/acs.joc.4c03107.

76 F. Juliá, Catalysis in the excited state: bringing innate transition metal photochemistry into play, *ACS Catal.*, 2025, **15**(6), 4665–4680, DOI: 10.1021/acscatal.4c07962.

77 R. Schmitt, A. Nenning, O. Kraynis, *et al.*, A review of defect structure and chemistry in ceria and its solid solutions, *Chem. Soc. Rev.*, 2020, **49**(2), 554–592, DOI: 10.1039/C9CS00588A.

78 K. Chang, H. Zhang, M. Cheng, *et al.*, Application of ceria in CO_2 conversion catalysis, *ACS Catal.*, 2020, **10**(1), 613–631, DOI: 10.1021/acscatal.9b03935.

79 T. Montini, M. Melchionna, M. Monai, *et al.*, Fundamentals and catalytic applications of CeO_2-Based Materials, *Chem. Rev.*, 2016, **116**(10), 5987–6041, DOI: 10.1021/acs.chemrev.5b00603.

80 H. Tsurugi and K. Mashima, Renaissance of homogeneous cerium catalysts with unique Ce(IV/III) couple: redox-mediated organic transformations involving homolysis of Ce(IV)–ligand covalent bonds, *J. Am. Chem. Soc.*, 2021, **143**(21), 7879–7890, DOI: 10.1021/jacs.1c02889.

81 Y. Lu and J. G. West, Chemoselective decarboxylative protonation enabled by cooperative earth-abundant element catalysis, *Angew. Chem.*, 2023, **135**(3), e202213055, DOI: 10.1002/ange.202213055.

82 S.-C. Kao, K.-J. Bian, X.-W. Chen, *et al.*, Photochemical iron-catalyzed decarboxylative azidation via the merger of ligand-to-metal charge transfer and radical ligand transfer catalysis, *Chem Catal.*, 2023, **3**(6), 100603, DOI: 10.1016/j.checat.2023.100603.

83 Z. Hu, H. Yuan, C. Ye, *et al.*, Iron-photocatalyzed decarboxylative coupling reaction of carboxylic acids with alkynyl bromides, *J. Org. Chem.*, 2025, **90**(27), 9431–9437, DOI: 10.1021/acs.joc.5c00753.

84 S. Tamaki, R. Kuwata, S. Wakita, *et al.*, Mixed-metal Ce-Zr-Mn clusters as photo-catalysts for decarboxylative functionalization of carboxylic acids, *Angew. Chem., Int. Ed.*, 2025, **64**(33), e202505639, DOI: 10.1002/anie.202505639.

85 M. O. Zubkov, M. D. Kosobokov, V. V. Levin, *et al.*, Photocatalyzed decarboxylative thiolation of carboxylic acids enabled by fluorinated disulfide, *Org. Lett.*, 2022, **24**(12), 2354–2358, DOI: 10.1021/acs.orglett.2c00549.

86 L. Qin, X. Zhang, H. Sun, *et al.*, Visible-light-induced decarboxylative alkynylation of carboxylic acids in batch and continuous flow, *Green Synthesis and Catalysis*, 2024, **5**(1), 20–24, DOI: 10.1016/j.gresc.2022.10.002.

87 C. Kim, J. Jeong, M. Vellakkaran, *et al.*, Photocatalytic decarboxylative pyridylation of carboxylic acids using in situ-generated amidyl radicals as oxidants, *ACS Catal.*, 2022, **12**(21), 13225–13233, DOI: 10.1021/acscatal.2c04417.

88 S. Fukuzumi and K. Ohkubo, Organic synthetic transformations using organic dyes as photoredox catalysts, *Org. Biomol. Chem.*, 2014, **12**(32), 6059–6071, DOI: 10.1039/C4OB00843J.

89 S. Vijayakrishnan, J. W. Ward and A. I. Cooper, Discovery of a covalent triazine framework photocatalyst for visible-light-driven chemical synthesis using high-throughput screening, *ACS Catal.*, 2022, **12**(16), 10057–10064, DOI: 10.1021/acscatal.2c02743.

90 M. Forchetta, F. Valentini, V. Conte, *et al.*, Photocatalyzed oxygenation reactions with organic dyes: state of the art and future perspectives, *Catalysts*, 2023, **13**(2), 220, DOI: 10.3390/catal13020220.

91 M. Majek and A. Jacobi Von Wangelin, Mechanistic perspectives on organic photoredox catalysis for aromatic substitutions, *Acc. Chem. Res.*, 2016, **49**(10), 2316–2327, DOI: 10.1021/acs.accounts.6b00293.

92 L. Xiong and J. Tang, Strategies and challenges on selectivity of photocatalytic oxidation of organic substances, *Adv. Energy Mater.*, 2021, **11**(8), 2003216, DOI: 10.1002/aenm.202003216.

93 M. V. Bobo, J. J. Kuchta and A. K. Vannucci, Recent advancements in the development of molecular organic photocatalysts, *Org. Biomol. Chem.*, 2021, **19**(22), 4816–4834, DOI: 10.1039/D1OB00396H.

94 J. D. Griffin, M. A. Zeller and D. A. Nicewicz, Hydrodecarboxylation of carboxylic and malonic acid derivatives via organic photoredox catalysis: substrate scope and mechanistic insight, *J. Am. Chem. Soc.*, 2015, **137**(35), 11340–11348, DOI: 10.1021/jacs.5b07770.

95 Y. Yu, W. Yuan, H. Huang, *et al.*, Visible-light-mediated decarboxylative alkylation cascade cyano insertion/cyclization of *N*-arylacrylamides under transition-metal-free conditions, *J. Org. Chem.*, 2018, **83**(3), 1654–1660, DOI: 10.1021/acs.joc.7b03080.

96 C. Shu, R. S. Mega, B. J. Andreassen, *et al.*, Synthesis of functionalized cyclopropanes from carboxylic acids by a radical addition–polar cyclization cascade, *Angew. Chem., Int. Ed.*, 2018, **57**(47), 15430–15434, DOI: 10.1002/anie.201808598.

97 M. M. Mastandrea, S. Cañellas, X. Caldentey, *et al.*, Decarboxylative hydroalkylation of alkynes via dual copper-photoredox catalysis, *ACS Catal.*, 2020, **10**(11), 6402–6408, DOI: 10.1021/acscatal.0c01742.

98 R. S. Mega, V. K. Duong, A. Noble, *et al.*, Decarboxylative conjunctive cross-coupling of vinyl boronic esters using

metallaphotoredox catalysis, *Angew. Chem., Int. Ed.*, 2020, **59**(11), 4375–4379, DOI: 10.1002/anie.201916340.

99 Y. Sun, F. Tan, R. Hu, *et al.*, Visible-light photoredox-catalyzed hydrodecarboxylation and deuterodecarboxylation of fatty acids, *Chin. J. Chem.*, 2022, **40**(16), 1903–1908, DOI: 10.1002/cjoc.202200143.

100 C. Kim, J. Jeong, M. Vellakkaran, *et al.*, Photocatalytic decarboxylative pyridylation of carboxylic acids using in situ-generated amidyl radicals as oxidants, *ACS Catal.*, 2022, **12**(21), 13225–13233, DOI: 10.1021/acscatal.2c04417.

101 D. E. Edmondson and T. P. Singer, Oxidation-reduction properties of the 8α-substituted flavins, *J. Biol. Chem.*, 1973, **248**(23), 8144–8149, DOI: 10.1016/S0021-9258(19)43205-5.

102 H. Ding, N. Yan, P. Wang, *et al.*, Synthesis of reverse glycosyl fluorides via organophotocatalytic decarboxylative fluorination of uronic acids, *Org. Chem. Front.*, 2022, **9**(10), 2808–2814, DOI: 10.1039/D2QO00133K.

103 T. Taeufer, M. A. Argüello Cordero, A. Petrosyan, *et al.*, Photophysical and electrochemical properties of pyrimidopteridine-based organic photoredox catalysts, *ChemPhotoChem*, 2021, **5**(11), 999–1003, DOI: 10.1002/cptc.202100159.

104 T. Taeufer, R. Hauptmann, F. El-Hage, *et al.*, Pyrimidopteridine-catalyzed hydroamination of stilbenes with primary amines: a dual photoredox and hydrogen atom transfer catalyst, *ACS Catal.*, 2021, **11**(8), 4862–4869, DOI: 10.1021/acscatal.0c05540.

105 A. Petrosyan, L. Zach, T. Taeufer, *et al.*, pyrimidopteridine-catalyzed photo-mediated hydroacetoxylation, *Chem.–Eur. J.*, 2022, **28**(57), e202201761, DOI: 10.1002/chem.202201761.

106 T. S. Mayer, T. Taeufer, S. Brandt, *et al.*, Photomediated hydro- and deuterodecarboxylation of pharmaceutically relevant and natural aliphatic carboxylic acids, *J. Org. Chem.*, 2023, **88**(10), 6347–6353, DOI: 10.1021/acs.joc.2c01664.

107 Y. Zhang, J. Qian, M. Wang, *et al.*, Ketones as ideal photocatalysts for decarboxylative fluorination and a competition with C(sp^3)-H fluorination, *Chem Catal.*, 2024, **4**(12), 101162, DOI: 10.1016/j.checat.2024.101162.

108 W. Hu and J. Deng, Photocatalytic decarboxylation of waste cooking oil for green and efficient biodiesel production and life cycle assessment, *Chem. Eng. J.*, 2025, **519**, 164955, DOI: 10.1016/j.cej.2025.164955.

109 S. R. Nasireddy, P. Sharma, K. Khanna, *et al.*, Visible-light-mediated decarboxylative (amino)alkylation of azomethine imines, *J. Org. Chem.*, 2025, **90**(15), 5226–5230, DOI: 10.1021/acs.joc.5c00159.

110 F. Lorenz, T. Peppel, M. Brasholz, *et al.*, Applicability of semiconductor photocatalysts in photoredox reactions: highlighting the performance of polymeric carbon nitrides in radical three-component couplings, *ChemCatChem*, 2025, **17**(7), e202401847, DOI: 10.1002/cctc.202401847.

111 L. Cheng, Q. Xiang, Y. Liao, *et al.*, CdS-based photocatalysts, *Energy Environ. Sci.*, 2018, **11**(6), 1362–1391, DOI: 10.1039/C7EE03640J.

112 B. Weng, M.-Y. Qi, C. Han, *et al.*, Photocorrosion inhibition of semiconductor-based photocatalysts: basic principle, current development, and future perspective, *ACS Catal.*, 2019, **9**(5), 4642–4687, DOI: 10.1021/acscatal.9b00313.

113 H. Garg, S. Patial, P. Raizada, *et al.*, Hexagonal-borocarbonitride (h-BCN) based heterostructure photocatalyst for energy and environmental applications: a review, *Chemosphere*, 2023, **313**, 137610, DOI: 10.1016/j.chemosphere.2022.137610.

114 X. Zeng, X. Bu, H. Chen, *et al.*, Regulation of charge transfer direction and key steps via Y modification of redox-active sites on borocarbonitride for photocatalytic CO_2 reduction, *Composites, Part B*, 2024, **287**, 111838, DOI: 10.1016/j.compositesb.2024.111838.

115 F. Chen, X. Lv, H. Wang, *et al.*, Weak-Field electro-flash induced asymmetric catalytic sites toward efficient solar hydrogen peroxide production, *JACS Au*, 2024, **4**(3), 1219–1228, DOI: 10.1021/jacsau.4c00076.

116 M. Zheng, W. Cai, Y. Fang, *et al.*, Nanoscale boron carbonitride semiconductors for photoredox catalysis, *Nanoscale*, 2020, **12**(6), 3593–3604, DOI: 10.1039/C9NR09333H.

117 T. Yuan, M. Zheng, M. Antonietti, *et al.*, Ceramic boron carbonitrides for unlocking organic halides with visible light, *Chem. Sci.*, 2021, **12**(18), 6323–6332, DOI: 10.1039/D1SC01028J.

118 J. Shi, T. Yuan, M. Zheng, *et al.*, Metal-free heterogeneous semiconductor for visible-light photocatalytic decarboxylation of carboxylic acids, *ACS Catal.*, 2021, **11**(5), 3040–3047, DOI: 10.1021/acscatal.0c05211.

119 C. Hao, J. Wen, H. Song, *et al.*, Visible light-driven self-heating photocatalytic decarboxylation of fatty acid over α-Fe_2O_3, *Appl. Catal. B Environ. Energy*, 2024, **354**, 124122, DOI: 10.1016/j.apcatb.2024.124122.

120 G. Vilé, M. M. D. V. Ibáñez, L. A. Cipriano, *et al.*, Photocatalytic C(sp^3)–C(sp^3) cross-coupling of carboxylic acids and alkyl halides using a nickel complex and carbon nitride, *Nat. Commun.*, 2025, **16**, 7016, DOI: 10.21203/rs.3.rs-4838220/v1.

121 S. Bishi, B. Sankar Lenka, P. Kreitmeier, *et al.*, g-C_3N_4 Photocatalyzed decarboxylative oxidation of carboxylic acids and the oxidation of alkenes and alkanes, *Adv. Synth. Catal.*, 2024, **366**(15), 3397–3403, DOI: 10.1002/adsc.202400117.

122 A. Jati, A. K. Mahato, D. Chanda, *et al.*, Photocatalytic decarboxylative fluorination by quinone-based isoreticular covalent organic frameworks, *J. Am. Chem. Soc.*, 2024, **146**(34), 23923–23932, DOI: 10.1021/jacs.4c06510.

123 L. Hu, R. Li, Y. Liu, *et al.*, Energy-efficient photothermal catalysis of rubber seed oil for the preparation of biofuel compounds, *Fuel*, 2021, **306**, 121683, DOI: 10.1016/j.fuel.2021.121683.

124 H. Yang, L. Tian, A. Grirrane, *et al.*, Enhanced fatty acid photodecarboxylation over bimetallic Au–Pd core–shell

nanoparticles deposited on TiO_2, *ACS Catal.*, 2023, **13**(22), 15143–15154, DOI: 10.1021/acscatal.3c03793.

125 Y. Guo, M. Fang, S. Yuan, *et al.*, Enhanced photocatalytic alkane production from fatty acid decarboxylation over sulfide-modified TiO_2 under mild conditions, *Chem. Eng. Sci.*, 2024, **299**, 120555, DOI: 10.1016/j.ces.2024.120555.

126 X. Li, H. Xu, C. Ku, *et al.*, Photocatalytic decarboxylative alkenylation of fatty acids for coproduction of linear α-olefin and hydrogen with high selectivity, *ACS Catal.*, 2025, 19192–19204, DOI: 10.1021/acscatal.5c04570.

127 Z. Chen, H. Zhou, Y. Liang, *et al.*, Controlling radical pathways via valence engineering of Rh/TiO_2 for selective jet fuel synthesis from biomass, *ACS Nano*, 2026, 5c19788, DOI: 10.1021/acsnano.5c19788.

128 Y. Jiang, G. Wang, M. Ma, *et al.*, $Fe\text{-}N_2$ single-atom sites unlocked ligand-to-metal charge transfer in semiconductor photocatalytic decarboxylation, *Nano Res.*, 2026, **19**, 94908469, DOI: 10.26599/NR.2026.94908469.